Strategies to improve hydrogen activation on gold catalysts

Strategies to improve hydrogen activation on gold catalysts

Nikolaos Dimitratos[1,2], Gianvito Vilé[3], Stefania Albonetti[1,2], Fabrizio Cavani[1,2], Jhonatan Fiorio[4], Nuria López[5], Liane M. Rossi[6], Robert Wojcieszak[7,*]

[1]*Dipartimento di Chimica Industriale "Toso Montanari", Alma Mater Studiorum Università di Bologna, Viale Risorgimento 4, Bologna 40126, Italy*
[2]*Center for Chemical Catalysis-C3, Alma Mater Studiorum Università di Bologna, Viale Risorgimento 4, Bologna 40136, Italy*
[3]*Department of Chemistry, Materials and Chemical Engineering "Giulio Natta", Politecnico di Milano, Piazza Leonardo da Vinci 32, 20133 Milano, Italy*
[4]*Technische Universität Dresden, School of Science, Faculty of Chemistry and Food Chemistry, Mommsenstr. 13, 01069 Dresden, Germany.*
[5]*Institute of Chemical Research of Catalonia, The Barcelona Institute of Science and Technology, Tarragona, Spain*
[6]*Departamento de Química Fundamental, Instituto de Química, Universidade de São Paulo, Av. Prof. Lineu Prestes 748, São Paulo 05508-000, SP, Brazil*
[7]*Univ. Lille, CNRS, Centrale Lille, Univ. Artois, UMR 8181 - UCCS - Unité de catalyse et chimie du solide, F-59000 Lille, France*

**Corresponding author. E-mail: robert.wojcieszak@univ-lille.fr*

ABSTRACT

Catalytic reactions involving molecular hydrogen are at the heart of many transformations in the chemical industry. Classically, hydrogenations are carried out on Pd, Pt, Ru, or Ni catalysts. However, the use of supported Au catalysts has garnered attention in recent years owing to their exceptional selectivity in hydrogenation reactions. This is despite the limited understanding of the physicochemical aspects of hydrogen activation and reaction on Au surfaces. Similarly, a rational design of new improved catalysts relies on better exploiting the hydrogenating properties of Au. This review analyses the strategies employed to improve hydrogen-Au interactions, from addressing the importance of the Au particle size to exploring alternative mechanisms for H_2 dissociation on Au cations and Au-ligand interfaces. These insights hold the potential to drive future applications of gold catalysis.

[H1] Introduction

Catalytic transformations involving molecular hydrogen (H_2) are named hydrogenations, and are common in the chemical industry. For a long time, it was believed that only certain metals, such as platinum (Pt), palladium (Pd), and nickel (Ni) possessed the catalytic ability to dissociate H_2 efficiently. These metals have been extensively used in industrial processes owing to their ability to facilitate hydrogenation reactions. However, issues related to overhydrogenation with Ni catalysts and the high cost and limited availability of Pt and Pd have prompted researchers to explore alternative catalysts. In this pursuit, scientists discovered that gold (Au), typically considered inert, can catalyze the activation of H_2 and other H-donors, and exhibit remarkable catalytic properties in hydrogenation reactions.[1-2] This finding has shattered a long-standing limitation in the field and opened up new possibilities for increasing the selectivity of various hydrogenation processes (BOX 1).

Heterogenous catalysts are used in many industrial processes[5-7], often involving finely dispersed metallic nanoparticles. One such catalytic system is Au nanoparticles (Au NPs) dispersed on solid carriers[8], which were initially demonstrated for selective CO oxidation reactions[9-11]. Dispersing the Au nanoparticles in this way provides a large number of low-coordination surface sites which offer improved catalytic properties over conventional Au surfaces[10,12]. This enhanced activity and selectivity are linked to the quantum effects unique to the nanoscale. When Au nanoparticles are very small (below <2 nm in diameter), significant quantization occurs to the conduction band. In these quantum-sized nanoparticles, many of the physical and chemical properties of Au are fundamentally altered.[13] For example, quantum-sized Au nanoparticles show multiple optical absorption peaks in the optical spectrum whereas a single surface plasmon resonance (SPR) peak at 520 nm is observed for larger spherical Au nanoparticles. In addition, removing or adding one Au atom can alter the electronic properties of Au nanoparticles owing to the strong quantum confinement effect.[13] Together with Au-support interactions, these quantum effects are responsible for the unusual catalytic properties of Au which allow Au NPs to activate small molecules such as carbon monoxide at low temperatures. The discovery that very small Au particles, specifically those with sizes smaller than 10 nm, can be a viable catalysts for hydrogenation reactions was a breakthrough in heterogeneous chemistry[14-16]. Understanding the mechanisms by which hydrogen can be activated on Au is crucial to designing stable and efficient supported Au catalysts for hydrogenation reactions[17-18].

Generally, hydrogenation reactions on metal surfaces, including Au, follow the Horiuti-Polanyi mechanism that involves the homolytic splitting of a hydrogen molecule adsorbed on the metal surface and the sequential transferring of each H atom to the reactive molecule. This critical activation step has been explored using Infra-red (IR), X-ray absorption fine structure (XAFS), and Hydrogen/Deuterium exchange experiments on supported Au NPs [2,19-21]. By combining theory and experiment, the nature and structure of the active sites responsible for the adsorption and dissociation of molecular hydrogen are now well understood. The presence of the low-coordinated atoms located at the corner and edge of the Au particle is necessary for H_2 splitting on Au NPs[2,19-22]. Hydrogen adsorption is only possible on low coordinated atoms whereas AuNPs become repulsive at high coordination numbers (>8). Despite these efforts, some key questions remain concerning the charge transfer between the Au surface and the adsorbed H species, the presence of alternative hydrogen dissociation paths, and the degree of

mobility of H species on the Au NPs[23]. The main challenge in using Au for hydrogenation reactions is its low efficiency in dissociating H_2 under standard conditions. The important factors that make bulk Au the most noble metal and ineffective for hydrogen dissociation owe to the largest orbital overlap with the adsorbed hydrogen and highly filled antibonding adsorbate-metal *d* states[24].

In this Review, we will discuss the main strategies to assess the hydrogenation activity of Au nanoparticles and single atoms. We will focus our discussion on strategies that can enhance Au–H interactions and thus improve the hydrogenation ability of Au. This review reports on hydrogenation and hydroconversion reactions using Au nanoparticles and single atoms. Specifically, we highlight the most substantial advances concerning hydrogenation on Au-based catalysts from the last 5 years. Following this, we identify challenges to the design of more efficient Au formulations for the selective hydrogenation processes in heterogeneous and single atom catalysis. Next, we discuss the chemical aspects of the catalytic reaction during the selective hydrogenation process and, finally, the theoretical aspects of hydrogenation on Au surfaces including hydrogen dissociation and transfer. We hope to contribute to advancing the understanding of the relationships between reactions involving H_2 and Au catalysts in the catalysis and materials chemistry communities.

[H1] Hydrogenations on Au

The fundamental development of Au based catalytic formulations[18, 25-27] and the enhancement of existing systems[28-30] require a deep understanding of the impacts of active metals, supports, solvents, metal additives, co-catalysts, catalyst preparation methods, and the study of active site. The catalytic performance of Au is substantially improved through the design of multi-phase formulations (bimetallic and promoted Au catalysts) as well as synthesis methodologies to enhance the active phase dispersion and modulate the size and localization of Au nanoparticles within a support material. Theoretical investigations have provided insights into the mechanism of H_2 activation, hydride formation,[31] and the adsorption of the substrates on both Au and oxide (playing role of the support) surfaces. Furthermore, these studies have contributed to the understanding of reaction mechanisms in these systems, from homolytic to heterolytic H_2 dissociation (BOX 2).

The development of Au catalysts remains hampered by a number of obstacles. For example, the ability to control and tune the chemical composition of Au and Au bimetallic nanoparticles and/or nanoclusters is limited, especially when catalysts are prepared with traditional methods such as co-precipitation or co-impregnation of metal salts. These procedures frequently allow for limited control over the size and uniformity of the particles, leading to the formation of mixed particles that consist of both mono- and bimetallic nanoparticles. Another problem is the deactivation of the catalyst from structure degradation, leaching, and carbon deposition[34]. The mechanisms underlying the degradation of the catalyst performances are still not fully understood and need additional attention to mitigate the deactivation. Finally, various fundamental aspects of the mechanism remain not completely understood, such as kinetic modelling, adsorption geometry and active phase modelling.

One motivation behind research into catalysis on Au is the potential to enhance the efficiency of hydrogenation reactions. The design of nanostructured supported Au catalysts allows the development of catalyst systems with high activity and selectivity, and excellent

resistance to both chemical and structural degradation. One of the crucial parameters of the catalyst design is the optimisation of the structure of the active sites to enhance catalyst selectivity in hydrogenation reactions[15-16]. In addition, while the mechanism of hydrogen adsorption on a pure Au surface is well established, the fate of hydrogen species after dissociation from the metal is not completely understood, including the degree of H atom mobility on Au particles[23]. Several uncertainities remain around the reactivity of specific Au atoms and the origin of the dissociation (activated or/and spontaneous). Theoretical investigations have helped to develop more efficient Au-based catalysts for hydrogenations, such as open surfaces as Au(100) and low coordinated sites (edges or defects) that enhance the Au activity[35].

A fundamental understanding of the interactions of hydrogen with Au as well as those between the Au-ligand and Au-support are necessary to rationalize the performance of the catalysts, from the nano to the single-atom catalysts (SACs) level[36-38]. For example, in the semihydrogenation of alkynes, Au was predicted to exhibit a higher selectivity to alkenes than Pd by Density Functional Theory (DFT) and it was also confirmed experimentally[35]. In hydrogenation on Pd catalysts, both triple and double C–C bonds are adsorbed at the same rate and thus the competition between both types of bonds occurs resulting in a mix of products[35]. Conversely, the triple C–C bonds of alkynes are preferentially adsorbed and are subsequently activated on Au[35]. That is to say that triple C–C bonds can be preferentially hydrogenated and the alkene products can desorb from the Au surface avoiding further hydrogenation[35]. This high chemoselectivity of supported small Au nanoparticles enabled the hydrogenation of α,β-unsaturated aldehydes to the corresponding unsaturated alcohols[39-40], and the deprotection of epoxides via deoxygenation to the corresponding alkenes[41], in both cases preserving the C=C bonds.

[H1] Improving Au-hydrogen interactions

The activation of hydrogen on Au (leading to its dissociation) is considered the rate-determining step in Au-catalyzed hydrogenations[24]. In this context, several strategies have been developed to enhance the rate of H_2 dissociation to improve the catalytic efficiency of supported Au catalysts (**Figure 1**). The main approaches are the heterolytic hydrogen dissociation occurring on Au interacting with nitrogen-containing ligands[42] **(Figure 1a)** or at the metal-support interface in case of strong metal support interactions (SMSI)[43] **(Figure 1b).** H_2 dissociation could be also induced by hot electrons generated by plasmon enhancement[44] **(Figure 1c)** or at single Au atoms (**Figure 1d**)[45], as well as by alloying gold with a second metal as schematically represented on **Figure 1f**. Here, we discuss the most important approaches to enhance the reactivity of Au on hydrogenations.

[H2] Ligands

Auxiliary ligands can help to enhance selectivity in heterogeneous catalysis. In hydrogenation on Au NPs, the addition of certain ligands has demonstrated enhanced activity in the selective hydrogenation of alkynes to *cis*-alkenes (**Figure 2a**). An inactive silica-supported Au nanoparticle catalyst (Au/SiO_2) exhibited a substantial increase of activity in the presence of various nitrogen-containing ligands[42]. In the presence of piperazine, for example, the Au catalyst gained activity and selectivity to the alkene, even when allowed to continue to full

conversion (**Figure 2b**), where most catalysts lose selectivity. Ligands with two nitrogen donors were more capable at decreasing the energy barrier (activation energy) for the heterolytic dissociation of H_2 and improved the Au hydrogenation reaction rate **(Figure 2d)**. Ligands with only one nitrogen donor (red squares in Figure 2d), such as pyrazine, are capable of splitting H_2, but do not show the same catalytic performance, because they easily leave the Au surface after protonation and do not complete the H-transfer steps required to complete the catalyst cycle. According to DFT studies, the ligand−Au interface is responsible for the H_2 dissociation through a heterolytic mechanism. First, the H_2 molecule approaches the ligand−Au interface. The H_2 molecule is cleaved heterolytically, the proton is transferred to the amine ligand, forming a quaternary N center, and the hydride goes to the Au surface. Then, the H species adsorbed on Au can be transferred to the adsorbed alkyne**.** The catalytic cycle is completed after the proton transfer from the ligand to the organic moiety, which regenerates the amine ligand, followed by desorption of the alkene. A number of experimental parameters needed to be optimized to achieve an effective hydrogenation reaction. This included identifying a ligand with optimal basicity for the lowest input energy for hydrogen activation, that did not bind too strongly preventing blocking of the catalyst site, and also did not cause metal leaching that affected the stability of the Au surface[42]. Piperazine was selected as the best ligand, among nineteen amines tested, to promote the catalytic hydrogenation of alkynes on Au NP catalyst[42]. The Au-ligand catalytic system can be considered a frustrated Lewis pairs (FLP) analogue[46]. Other studies in the literature showed similar observations when combining Au NPs either with other nitrogen-containing[47-48] and phosphorous-containing[49] ligands for hydrogenations.

It is noteworthy that the presence of nitrogen atoms in graphitic carbon materials (N-doped carbon) prepared through 1,10-phenanthroline pyrolysis has shown a similar effect reported above on the properties of Au nanoparticle catalysts, specifically in catalytic hydrogenation reactions. The basic N atoms of the carbon support play an importan role for the hydrogen activation (in heterolytic mode) at the Au-N-doped carbon interface. In this context, Au nanoparticles coated with N-doped carbon materials supported on titania (Au@N-doped C/TiO_2) showed an enhanced catalytic activity (**Figure 2c**) when compared to uncoated Au/TiO_2 for alkyne semihydrogenation[47]. The main advantage compared to the previous study, is that the catalyst is fully heterogeneous, meaning it can be reused and the products easily separated by filtration. The nitrogen atoms present in the carbon material are part of the catalyst's composition and do not need to be added, as external ligands, like in the previous study[5]. A combination of experimental and computational studies revealed a N-assisted heterolytic H_2 activation mechanism (**Figures 2e**). The creation of an interface that mimicked the N-doped (pyridinic) graphene-like sheets experimentally observed after pyrolysis, revealed a behaviour similar to an FLP that enables a essentially barrierless heterolytic dissociation of H_2 (**Figure 2e**, TS-C). The FLP is formed due to the absence of a direct interaction between Au and the lone pair of the nitrogen, allowing a unique interface that promotes the heterolytic cleavage of H_2[47]. Then, the catalytic cycle is completed by two H-transfer steps (**Figure 2e**, TS-D and TS-E) and product desorption, closing the catalytic cycle and regenerating the initial species A. The mechanism illustrates the major role of N-heteroatoms on the H_2 activation.

In another example, verified by DFT calculations, Lewis bases, such as NH_3, adsorbed on four different models for Au surfaces and clusters (Au(111)-close-packed, Au(211)-step-edged, Au(111)-single atom, and Au_{38} cluster) were able to generate hydrides (H*) and protons (NH_4*)

through heterolytic H_2 dissociation. The generated hydride and proton can then be concertedly transferred to CO_2 to produce formic acid in all four Au models[50]. The cooperation between Au and adsorbed basic ligands has also been employed in the hydrogenation of other organic molecules, including quinolines[51], imines or nitriles[48] and aldehydes[52-53].

[H2] Au-support interactions

Another strategy to enhance the hydrogenation activity of Au is to exploit strong metal-support interactions (SMSIs). SMSIs refer to the interactions that occur between metal nanoparticles or atoms and the support material in heterogeneous catalysts[29-30]. These interactions play a critical role in the performance and stability of the catalysts and are particularly important for catalysts supported on oxides, such as SiO_2, Al_2O_3, or TiO_2. In catalysis, SMSIs can lead to several effects such as promotion of the dispersion of metal nanoparticles on the support, preventing their aggregation and leading to a higher surface area and more active sites. They enhance the stability of the metal nanoparticles on the support, preventing their sintering or leaching during the catalytic process[30]. In addition, SMSIs can influence the adsorption and activation of reactant molecules, affecting the selectivity of the catalytic reaction. Thus, by exploting SMSIs, the support stabilizes heterolytically dissociated hydrogen. This outcome arises from the intimate proximity between the support and the metal catalyst **(Figure 1b)**, fostering charge redistribution and electronic polarization. In hydrogenations, these factors collectively contribute to the enhanced stability of the dissociated hydrogen species. Compared to homolytic dissociation, heterolytic dissociation is much more energy intense, as determined experimentally (4.52 eV vs 17.36 eV)[54-55]. Thus, the extra energy needs must be compensated via the creation of new bonds, setting a minimum level of charge separation for the process to occur efficiently[54]. The interface of the oxide support can help to enhance this heterolytic process[43, 56]. An illustration of this concept can be observed in the case of TiO_2(110), where the presence of low coordinated O_2 atoms adjacent to the Au clusters has been observed. This arrangement has the potential to facilitate the dissociation of molecular H_2, leading to the protonation of the oxygen atoms situated on the support[56].

In contrast, the Au SACs supported in electron-rich cavities of N-doped carbon (such as graphitic carbon nitride obtained by the pyrolysis of organic amines– C_3N_4) dissociate H_2 homolytically[45]. The catalyst was suggested by DFT to be composed of $Au^{\delta+}$ ($1<\delta<3$) species stabilized in oxidized-4-pyridine cavities from the N-doped carbon. The developed catalyst led to thermodynamically more favored H_2 activation than the stepped surface Au(211) (−1.13 eV versus −0.17 eV, respectively).

The structure-sensitivity (the kinetics is dependent on the particle size due to changes in the coordination of surface atoms with particle size) of Au can also promote catalysts. Small Au NPs supported on TiO_2 of around 3 nm exhibited a higher selectivity to 3-vinylaniline (78%, side product being 3-ethylnitrobenzene with 16%) than the those of 9 nm (39% of 3-vinylaniline and 51% of 3-ethylnitrobenzene) in the hydrogenation of 3-nitrostyrene. In addition, a model catalyst containing both Au particle sizes (3 nm and 9 nm) showed a moderate selectivity to 3-vinylaniline (55%) at relatively high conversion (25%)[57]. Nevertheless, the application of a reduction process to the Au catalysts resulted in an enhanced selectivity for both particle sizes. In both cases, with particle sizes of 3 nm and 9 nm, the selectivity surpassed 95% after the

reduction process. The main difference was that the catalyst with the larger Au nanoparticles (~9 nm) exhibited a substantially lower conversion (14.9%) than the catalyst with 3 nm Au NPs (or combination of 3 and 9 nm, 15.4 and 24.8% respectivelly) which maintained a high conversion level[57]. By characterizing the catalysts by high resolution transmission electron microscopy (HRTEM), it was found that the catalyst with the larger Au nanoparticles (9 nm) had a larger degree of encapsulation, which reduced the catalytic activity. For smaller Au nanoparticles, only partial encapsulation was observed. This was explained by the surface tensions of the metal and support during the encapsulation process[57]. Typically, the metal has a higher surface tension than the TiO_2 support, which is often observed experimentally. In the case of Au, its relatively low surface tension ($\gamma Au = 1.51\ J\ m^{-2}$) has been considered as a hindrance for the formation of SMSIs[57]. Recent discoveries of SMSIs in TiO_2 supported Au catalysts have challenged the previously reported surface tension of TiO_2 (1.3–1.9 $J\ m^{-2}$) and raised questions about its potential overestimation[58]. This opens up the possibility that Au may possess a higher surface tension than TiO_2, allowing it to be wetted by TiO_2, and leading to the encapsulation of Au nanoparticles as a result of the minimization of their surface free energy. Furthermore, at the nanoscale, the size-dependence of surface tension plays a significant role. While both positive and negative correlations between surface tension and particle size have been observed, a positive correlation is more likely at high temperatures owing to the non-negligible contribution of surface entropy. A higher degree of encapsulation can be obtained for larger Au nanoparticles because their higher surface energy facilitates their wetting by TiO_2[57].

An alternative strategy to enhance the hydrogenation activity of Au uses uniform Au NPs decorated with carbon atoms. Located in the interstitial positions in the lattice, carbon atoms can strongly affect the electronic properties of Au. The Au NP catalytic performance was investigated using synthesized Au interstitial nanocatalysts supported on ordered mesoporous carbonaceous materials (C–Au/OMC) and commercial catalysts (Au supported on SiO_2 and activated carbon)[59]. The material with interstitial carbon species showed an improved catalytic performance and a high selectivity (well beyond 99%) compared to commercial catalysts. To understand the observed catalytic trend, DFT and XPS studies were carried out. The presence of interstitial C enables the activation of H_2 molecules. Specifically, the electron transfer between C and Au leads to the heterolytic dissociation of H_2 on the C–Au interface. The unique adsorption configuration of C–Au further influences the chemisorption process due to its distinct electronic properties. This selective adsorption and activation of H_2 on Au surfaces containing interstitial C, as compared to pure surfaces, explains the remarkable chemoselectivity observed for the C–Au/OMC catalysts when compared to commercial Au/C and Au/SiO_2 catalysts[59]. Additionally, there may be a continuous exchange of C atoms between the surface and subsurface, potentially facilitating the adsorption of H_2 molecules. Moreover, in case of the 3-nitrostyrene hydrogenation on Au supported mesoporous carbon catalysts high chemoselectivity to 3-vinylaniline was observed[59]. This was attributed to the perpendicular adsorption of the substrate, stronger interaction of the 3-nitrostyrene with the C containg Au surface and its enhanced activation on it. It was concluded that the high d-electron transfer from C to Au due to the C-Au interactions promotes the activation of the 3-nitrostyrene on the C-Au interface. This enhanced H_2 dissociation improved the catalytic performance of the Au NPs in hydrogenation reactions[59].

[H2] Plasmon enhancement

Exploiting the plasmonic properties of Au NPs (localized surface plasmons, LSPR) is an alternative strategy to activate H_2[23,44,60]. Here, hot electrons are formed from light illumination which then relax or scatter, initiating the catalytic hydrogenation reaction. Hot electrons are high-energy electrons produced through the interaction of light with metallic nanoparticles or nanostructures, and are being explored in new and exciting applications within nanotechnology and photonics. For catalysis, using hot electrons decreases the energy barrier for H–H activation owing to the transfer of electrons to the antibonding orbital of hydrogen[44]. Hot electrons induced dissociation of hydrogen on small Au particles. When a Au NP is exposed to light with sufficient energy (e.g., visible light), absorbed photons excite electrons in the Au to higher energy levels. These hot electrons have excess energy compared to the equilibrium Fermi level of Au. This excess energy can be transferred to hydrogen molecule and provide the activation energy required to activate H_2 molecules. Small Au supported on SiO_2 nanoparticles prepared by chemical deposition precipitation method were used in H_2 dissociation experiments (**Figures 3a-c**). **Figure 3a** illustrates the rate of H–D formation on the Au/SiO_2 photocatalyst both with and without supercontinuum laser excitation. Initially, the photocatalyst was maintained in the dark at 22−24 °C, yielding a constant background H–D level (**Figure 3a**)[60]. Upon laser activation, the rate of H–D generation immediately surged by approximately 150 times. This heightened rate stabilized within 10 minutes of laser stimulation. Concurrently, the sample's temperature rose by roughly 8 °C (up to 30°C) due to laser-induced heating (**Figure 3a**). After 10 minutes, the laser was deactivated, promptly restoring the system to its initial rate and temperature, showcasing the process' reversibility[60]. For a direct comparison of H_2 dissociation efficiency between the Au/SiO_2 and Au/TiO_2 photocatalysts, **Figures 3b and 3c** display the monitored photocatalytic H–D formation rates for both catalysts. In contrast to the approximately 150-fold increase observed for Au/SiO_2 (**Figure 3b**), the enhancement in the case of Au/TiO_2 (**Figure 3c**) was modest, measuring around 2.7 times. The subdued rate for Au/TiO_2 may be attributed to the formation of a Schottky barrier (with a nominal height of 0.8−1 eV) at the Au−TiO_2 metal-semiconductor junction. During laser excitation, hot electrons possessing energies surpassing the barrier's height can effectively transfer from the Au nanoparticles to the TiO_2, contributing to the observed effects[60]. As the rate of hydrogen dissociation decreased substantially when SiO_2 was replaced by TiO_2, (**Figures 3b-c**) indicates that H_2 dissociation occurring on the illuminated AuNP surface and the dielectric oxide is not participating in the process.[60] A key challenge remains in the diffusion of hydrogen through the support and its recombination, which is essential to understanding the activity of hydrogen on a Au surface. The redshift in the Localized Surface Plasmon Resonance (LSPR) of Au nanoparticles is attributed to the charge transfer between Au and hydrogen atoms during hydrogen adsorption and diffusion. The charge transfer induces alterations in the properties of the Au nanoparticles, causing a redshift in the LSPR. The observed red-shifted intensities are closely linked to variations in the sizes of the Au nanoparticles, suggesting that hydrogen atoms predominantly adhere to specific facets or flat surfaces of the Au particles. H atoms may also recombine at this site and desorb into the gas phase again[23]. The measured LSPR shifts was of about 0.02 nm during H_2 adsorption (as messured by Transmittance Anisotropy

Spectroscopy)[23]. Hydrogen chemisorption occurred directly on Au. Furthermore, the relationship between the redshift intensity and the size of nanoparticles indicates that dissociated hydrogen (H) atoms migrate across the NP surfaces, predominantly on the (100) facets. These atoms subsequently recombine and desorb into the gas phase. Under atmospheric pressure of H_2, an average negative charge transfer of approximately -0.06 electron charge units from each surface Au atom to hydrogen (H) occurs, with a localized charge back-bonding estimated to be around -0.2 electron charge units for each Au-H bond. Consequently, these results confirmed, in line with theoretical studies, that after H adsorption the electron population in Au nanoparticles decreases[23]. This enhanced comprehension of the chemisorption mechanism of H_2 onto Au NPs is anticipated to facilitate advancements in the fabrication and utilization of catalytic Au NPs for hydrogenation reactions[23].

In photocatalytic reactions, Au NPs have exhibited unique catalytic properties, even at low temperatures or low light intensity. This suggests that the use of Au photocatalysts in chemical reactions governed by mechanisms involving plasmonic effects and hot electron transfer may also be advantageous[61-63]. This is espacilly true for hydrogenation reactions were the hydrogen dissociation is often one of the limiting steps, as discussed above in the case of the photocatalytic hydrogen dissociation and H–D formation. The hot electrons transferred to H_2 were vital for high yields and the plasmon decay substantially lowered the energy barrier for hydrogen dissociation[60]. Moreover, the dissociation of H_2 on the Au surface under visible light excitation opens up the possibility of developing more effcient catalysts for the hydrogenation processes. For example, increased chemoselectivity was reported for the semi-hydrogenation of phenylacetylene under visible light irradiation using a nano-designed hybrid catalyst composed of plasmonic core (Au or bimetallic Au@Ag) and Pt shells compared to classical Au supported SiO_2 catalysts[64].

To increase the catalytic performance of non-plasmonic metals like Pt, a successful integration of plasmonic and catalytic properties is required. The most widely used approach to achieve this is by harnessing the hot carriers generated through LSPR excitation. These hot carriers play a pivotal role in enhancing the catalytic activity of the material. Au NPs supported on SiO_2 and TiO_2 showed both negative (reduced reaction rate) and positive (catalytic enhancement) effects for 4-nitrophenol hydrogenation under visible-light illumination. The difference in plasmonic catalytic activities[65] were attributed to the charge transfer at the interface of Au and the support as well as to the reducing agent (H_2 and $NaBH_4$) used during the catalyst synthesis. Au/SiO_2 NPs were substantially more active under plasmon excitation, while Au/TiO_2 catalysts were only enhanced by plasmons when H_2(g) was used as reductor. Reduced reaction rate observed upon reduction with BH_4^-(aq) was attributed to the transfer of hot electrons from Au to TiO_2.

[H2] Cationic Au

An alternative approach for improving the activation of hydrogen is by using dispersed cationic Au species, in which isolated Au ions are dispersed throughout a carrier. The synthesis of these type of material is not trivial and usually requires several steps as illlustrated in **Figure 4a**. In case of gold supported on carbon nitride two most important steps are linked to the thermal treatment, firstly at low (686°C) and then at high temperature above 1246°C (**Figure 4a**). This structure resembles traditional organometallic catalysts[66-71], comprising isolated

metals that are bonded to organic ligands (**Figure 4b and Figure 1e**). These structures are also described as single-atom catalysts (SACs), which are attracting growing interest because they can make better use of the metal phase compared to standard metal nanoparticles, and have provided excellent levels of selectivity, activity, stability in hydrogenations[72-76]. Cationic Au single-atom catalyst (Au SACs) decorated on multiwalled carbon nanotubes provided a highly efficient hydrogenation of 1,3-butadiene and 1-butyne under parahydrogen (an isomeric form of molecular hydrogen)[77]. Atomically dispersed Au catalyst provided a better selectivity and activity in the pairwise addition of hydrogen than the supported Au NPs catalysts. Similarly, isolated Au species (Au^+) supported on iron oxide (FeO_x) showed higher resistance to sintering (increase of the particle size) compared to other Au nanostructures for alkene hydrogenations[78-82]. Theoretical studies revealed that surface-anchored Au^+ species provided very high stability and improved catalytic activity compared to other Au nanoparticle catalysts, because of the covalent Au-support interactions. For example, a supported Au(III) species anchored on the MgO surface induced high activity and selectivity in ethene hydrogenation[79]. The conversion of ethene strongly depended on Au–Au coordination number (**Figure 4c**). The Au NPs were less efficient catalysts for ethene hydrogenation than Au SACs, and the atomic dispersion of the active phase (in SACs) was beneficial to drive the hydrogenation catalysis[79].

The developments in SAC design were made possible by advances in atomic-resolution microscopy that can image the dispersed metal atoms and their evolution under reaction conditions[83-84]. However, the practical use of Au SACs is often compromised by challenging synthesis protocols, including the use of aqua regia as a dispersing agent, as well as low resistance to sintering for non-functionalized carbon materials under reaction conditions[43]. To address the difficulty of making such materials, a co-precipitation strategy can be applied[85]. Here, the metal is added during synthesis of the metallic organic framework (MOF) precursors, intercalated through the layers *via* electrostatic surface interactions replacing anions present in the MOF structures (for exemple sulfate ion). The positively charged Au atoms were detected using high-angle annular dark-field STEM imaging (HAADF-STEM) and extended x-ray absorption fine structure (EXAFS) measurements. This approach draws analogy with the copolymerization route used for the immobilization of isolated atoms on graphitic C_3N_4[86-87]. Au-SACs prepared by co-precipitation methods were tested in the hydrogenation of *p*-nitrophenol to *p*-aminophenol and showed improved activity compared to classically prepared MOFs[85]. In addition, after 10 catalytic cycles, the catalyst retained its original morphology and activity, indicating an excellent stability.[85]

A kg-scale synthesis of Au_1/CeO_2 SAC was reported using a dry ball milling synthetic protocol[88]. This catalyst was then tested in the hydrogen oxidation (1 vol% H_2 + 1 vol% O_2 balanced with He). In the latter, the catalyst showed only ~10% of hydrogen conversion at 160 °C[88]. Despite a modest yield, this approach demonstrates that a proof of concept that noble metal supported SACs can be prepared at large scale using a facile and reproducible methodology.

[H2] Alloying and bimetallic synergy

Hydrogen dissociation can also be improved by exploiting Au alloying to generate weakly bound H atoms [89-91]. Ideally, an alloy structure (**BOX 3**) should effectively combine one metal (Pt-group metals and metals in the Pd and Pt triads especially) that promotes

hydrogen dissociation and another (Au, Cu or Ag) that can react with the dissociated H atoms and therefore promote hydrogenation[104-105]. The most promising bimetallic catalysts for processes involving hydrogen are Au–Pd nanoparticles in either an alloy where the two different metals are homogeneously arranged or in a core-shell structure when one metal is at the core and the second metal forms the shell[106]. The optimal ensemble configuration for heterolytic H_2 activation remains up for debate. In Au–Pd alloys with a controlled density of Pd atom ensembles in the surface (monomers, dimers, trimers) the presence of neighboring Pd atoms is crucial for hydrogen activation. That is, the ensemble must be at least a dimer as Pd monomers are not able to adsorb hydrogen[107].

It is important to identify the sites responsible for the activation of H_2 in Au–Pd alloyed systems. This facilitates not only the identification of the minimal Pd ensemble (quantity of Pd needed to catalyse a reaction with optimal efficiency) for the activation of H_2 but also to reveal the energy profile for the spillover and release of hydrogen. The hydrogen spillover effect (HSPE) is an interfacial phenomenon in which active H atoms generated by the dissociation of H_2 on one phase (metal surface) migrate to another phase (support surface) and participate in the catalytic reaction of the substance adsorbed on that site. By modelling Au−Pd systems, it was anticipated that Pd atoms in a (111) surface of Au could activate H_2[94]. By combining TPD and high-resolution STEM it was shown that the a low number of isolated atoms of Pd are responsible for hydrogen dissociation. The quantity of surface atoms of Pd in Au reflects the number of H atoms adsorbed on the surface. Further TPD-H–D exchange and DFT studies provided the energetic landscape for the adsorption of H_2 including an understanding of the activation and desorption of hydrogen from isolated Pd atoms, the typical reaction pathway for activating H_2 and the mechanism of the release of hydrogen along the Pd atoms with minimum spillover of hydrogen species to the Au[95].

Using spatially resolved tip-enhanced Raman spectroscopy (TERS)[108-110], a study of the catalytic hydrogenation of chloronitrobenzenethiol to chloroaminobenzenethiol (**Figure 5a**) over Au–Pd catalyst was carried out[110] (**Figures 5 a-f**). TERS studies the topography and chemical composition of a surface with high accuracy and an excellent resolution of ~10 nm. To gain a more comprehensive understanding of the chloronitrobenzenethiol hydrogenation process, a quantitative characterization of the relationship between the active regions (blue regions on **Figures 5 c and e**) and surface structures was conducted[110]. In **Figures 5 d and f**, two distinct regions, each measuring 100 nm in width, featuring Pd islands (**Figure 5d**) and Au craters (**Figure 5f**) in the TERS maps are represented. Co-localized scanning tunneling microscopy (STM) images with accompanying height profiles are also given (as inserts in **Figure 5d and f**). In these representations, the active region is highlighted in light blue, while the non-reactive region is depicted in light red. In the case of Pd_{LC}/Au (Au surface with low Pd coverage, **Figure 5c and d**), the size of the active regions, is approximately 50 nm[110]. However, the size of the Pd islands within both regions measures only 20 nm. Conversely, for Pd_{HC}/Au (Au surface with high Pd coverage, **Figure 5e and f**), the active regions are approximately 15 nm larger than the Pd layer itself. The results reveal that the active regions extend approximately 15-30 nm beyond the boundaries of the Pd areas, where hydrogenation reactions occur. These spillover regions, however, exhibit an asymmetrical relationship with the shape of the Pd islands **(Figure 5c)**[110]. The obtained results revealed that hydrogenation takes place beyond the Pd active sites and was initiated by the spilt-over hydrogen dissociated on Pd. After dissociation

on Pd, hydrogen atoms migrated to adjacent Au surfaces over relatively long distance of 15-30 nm[110]. The mechanism of this hydrogenation involving hydrogen spillover was also determined by DFT and confirmed the feasibility of the long-distance diffusion and explained the enhanced chemoselectivity to the reactant in the Au–Pd bimetallic.

Single-atom alloys (SAAs) are a class of single-site catalysts in which small amounts of isolated metal atoms are present in the surface layer of a metal play the role of the host[104-105, 111-112]. Typically, SAAs are comprised of single atoms of a catalytically active metal alloyed into the surface of a less reactive host metal. For example, for the hydrogenation of butadiene to butene, hydrogen is dissociated at isolated metal sites, for example Pt, and the hydrogen atoms spill over onto the the host metal, such as Cu, where the reactant (butadiene) reacts to form the product (butene). This then desorbs prior to complete hydrogenation, demonstrating the chemoselectivity of this catalyst[105]. Such materials have also drawn interest owing to their potential to break linear scaling relationships in alloy catalysis. Under standard conditions (low temperature) Au is not able to activate hydrogen, however using SAAs of Au, highly selective hydrogenation reactions are enabled, such as selective hydrogenation of 1-hexyne to 1-hexene using Au–Pd SAA catalyst (**Figure 5 g and h**). The facile activation of hydrogen on Pd is possible using Au–Pd SAAs, where Au is incapable of dissociating molecular hydrogen[112]. To overcome this limitation, addition of small amounts of Pd to form a Au–Pd SAA has been reported to activate molecular hydrogen, although the dissociated hydrogen does not spill over onto the Au host[111]. In operando spectroscopy studies confirmed that the transformation occurs by first dissociating H_2 and splitting of the hydrogen species on the Pd sites followed by the reaction of the adsorbed H species on Au[111]. Moreover, by DFT studies performed on Pd–Au(111) surface, it was shown that C atom is bound to the Pd atom. Because the H atom is also bound more strongly to the Pd atom, it is more kinetically favorable to hydrogenate this mid-compound C atom than a terminal C atom. This considerably limits over-hydrogenation and oligomerization side reactions.

In bimetallic nanoparticles the chemical composition and order affect the catalytic properties of bimetallic systems[113]. The incorporation of a second metal can help to overcome the limitations observed for monometallic nanoparticles such as redox properties, stability and substrate adsorption. DFT predicted that by overcoming the size dependent relationship on monometallic Pt catalysts, a monolayer of Pt and Au catalyst would lead to higher activity as well as higher chemoselectivity in the hydrogenation of halonitrobenzenes[26]. As such, an Au@Pt/SiO_2 core-shell structure with a monolayer (ML) Pt shell was prepared using atomic layer deposition (ALD) methodology. In addition, the catalytic activity of a range of bimetallic Au–Pt catalysts using 0.5, 1 and 2 ML Pt shells, with 1 ML of Pt shell **(Figure 6a)** were compared in terms of the selectivity to *para*-chloroaniline[26] **(Figures 6b)**. The core-shell structure was confirmed using high resolution microscopy (**Figure 6c**) and reveled the Pt shell thicknes of about 0.3 nm (blue line in **Figure 6c**) in case of Au@1ML-Pt catalyst. The Au@Pt/SiO_2 catalyst exhibited a high catalytic activity (**Figure 6b**) owing to the enhanced charge transfer between Au and Pt atoms facilitated by the substantial ligand effect. The ligand effect can have a profound impact on the catalytic activity and specificity of the catalyst as the ligands can bind to the metal surface, and significantly modify its electronic and steric properties. The DFT studies also confirmed the terrace sites responsible for high selectivity were preserved[26], which improves the stability of the catalyst. These flat nanoparticle surface

regions with regularly arranged atoms play a vital role in catalysis by providing stable and well-defined surfaces for chemical reactions. Finally, the catalyst presented high stability compared to the monometallic Pt catalyst, that generally suffers from the agglomeration and leaching of Pt particles and chlorine poisoning[25].

Au-based bimetallic catalysts were also shown to possess excellent CO_2 hydrogenation activity, forming CO. For example, Ni–Au bimetallic catalytic systems based on core-shell structure are very active in this reaction[102] (**Figure 6d**). SiO_2 was chosen as a support of the core-shell nanoparticles, consisted of a *fcc* (*face centered cubic* structure in which atoms are arranged at the corners and center of each cube face of the cell) Ni core and Au shell formed by 2-3 atomic layers (**Figure 6d**).-Catalytic studies showed the Ni–Au bimetallic catalyst provided a high selectivity to CO (95%) with a conversion of 4.5-18% in the temperature range of 340-600 °C[102] (**Figure 6e**). *Ex situ* STEM characterization showed the presence of core-shell structure, with an ultrathin Au shell. However, during *in situ* STEM imaging, a phase transition was observed with the creation of a new Au–Ni alloy phase at similar reaction temperatures. In addition, *in situ* TEM analysis revealed that during the heat treatment from 450- 600 °C the Au species at the outmost surface were dissolved in the Ni matrix forming an alloy[102] (**Figure 6d,** top part). However, during the cooling process to 450°C, the dealloying process occurred and Ni@Au core shell structure was recovered (**Figure 6d**, bottom part). Control experiments carried out in a gas-cell reactor minimized the 'pressure gap' observed between the *in situ* environmental TEM measurements (~9 mbar) and the actual reaction conditions (1 bar) and reproduced the reaction-driven alloying of Au–Ni NPs, which confirmed the credibility of their original TEM results. Finally, DFT calculations confirmed the most energetically favoured reaction pathway, which consisted of two stages. The first was CO_2 hydrogenation to form adsorbed CO and the second was the diffusion of CO adsorbed on Ni to the Au sites and finally the desorption of CO **(Figure 6f)**. These results confirmed that the Ni active sites were responsible for the CO_2 hydrogenation and the Au active site for the high selectivity CO formation[102]. These results confirmed the alloying-dealloying mechanism occurred in the bimetallic Au–Ni systems. This is also the case of Au–Pd alloys. Pretreatment in oxygen leads enhances the activity in dilute Au–Pd alloys by bringing Pd to the surface of the Au particle. In the contrary, during the hydrogen treatment the Pd returns to the bulk and the catalyst suffers from deactivation[96-97].

[H1] Conclusion and Outlook

Au-based nanomaterials remain promising catalysts for selective hydrogenation reactions. The hydrogen activation pathway can be promoted in catalytic hydrogenations in four ways: assistance from light, the size of the metal nanoparticles, the Au-support interaction, and the presence of ligands or modifiers on the metal surface. Additionally, exploring the two activation modes (homolytic scission to H atoms or heterolytic scission into H^+/H^- pairs) in turn can make these catalytic processes more efficient. For example, to perform selective hydrogenations, organic linkers must be present on the Au surface to promote heterolytic scission.

Two key challenges in the development of Au-based nanomaterials for hydrogenation catalysts are the need to control the sintering of the Au species during reaction as well as the low solvent tolerance of these catalysts. Research continues in the search for appropriate

promoters and components able to enhance the catalytic activity of supported Au catalysts. The choice of promoter depends on the specific catalytic reaction and the desired enhancement in catalytic properties. Promoters play a crucial role in tailoring the activity, selectivity, and stability of Au nanoparticles for various applications in catalysis. Some of most important being organic ligands, sulfur containing species, metals and oxides (especially for core-shell structures). Moreover, shifting from neutral Au nanoparticles to cationic Au single atoms appears to improve the catalysts durability and open new pathways for the regeneration of the catalysts[114].

Another important challenge will be the use of hybrid catalysts mixing single atoms and nanoscale particles[115-117]. In this case, cascade reactions may be performed or the reaction rate can be substantially improved. This could be a useful parameter to explore in reactions involving hydrogen as the hydrogen dissociation and reactivity strongly depends on the size of the Au particle.

Finally, we need an improved fundamental understanding of the hydrogenation mechanisms as this should provide information for the rational design of new Au catalysts. To better understand the catalyst reduction process, and the nature and formation of intermediates, advanced *in-situ* characterization techniques will be required. The main issues are still linked to the very small size of acive Au species. The use of synchrotron facilities is required to fully characterize these materials. However, these facilities are in high demand among researchers from various scientific disciplines, including physics, chemistry or materials science. In situ techniques are also challenging as very often these experiments require extended setup and data collection times owing to their complexity. A crucialfactor often neglected is also the very first atomic layer in case of bimetallic nanoparticles. Probing the core and surface composition of nanoalloys to rationalize their selectivity is of high importance for understanding their catalytic selectivity. Characterization methodology must be developed to distinguish between the surface and core composition. Identification of the optimal balance between the two metals will help to tune the relative rates of various reaction pathways and, consequently, control the selectivity of the catalytic process. A combination of experimental analysis and DFT simulations will also be required to understand the adsorption-desorption process and the selectivity path to a specific product.

In summary, by adopting a multidisciplinary approach (material sciences, physics, chemistry, biology, and engineering) as well as leveraging advanced characterization and computational methods, researchers can explore future applications of Au-based materials. The integration of advanced characterization techniques and computational methods enhances our understanding and paves the way for new advances. Gold-based materials, when viewed through this multidisciplinary lens, hold immense promise, not only in hydrogenation processes but also in other domains. Beyond their traditional roles, these materials have emerged as catalysts in the realm of sensing technologies, enabling novel possibilities for detecting and responding to various stimuli. Moreover, in the field of nanomedicine, Au-based materials may contribute to advances in diagnostics and therapies. As nanocarriers, they have the potential to stand at the forefront of innovative drug delivery systems, offering tailored solutions for precision medicine and revolutionizing the landscape of therapeutic interventions. Au-based materials are poised to be versatile tools across a spectrum of applications that transcend disciplinary boundaries.

604

Acknowledgements

R.W. discloses support for publication of this work from Programme Investissement d'Avenir [I-SITE ULNE / ANR-16-IDEX-0004 ULNE], Métropole Européenne de Lille (MEL) and Region Hauts-de-France for the [CatBioInnov project].

Author contributions

The authors contributed equally to all aspects of the article.

Competing interests

The authors declare no competing interests.

Peer review information

Nature Reviews Chemistry thanks Mathilde Luneau, Hio Tong Ngan, Philippe Sautet, and the anonymous reviewers for their contribution to the peer review of this work.

References

1. Wood, B. & Wise, H. The role of adsorbed hydrogen in the catalytic hydrogenation of cyclohexene. *J. Catal*. **5**, 135-145 (1966).
2. Fujitani, T.; Nakamura, I.; Akita, T.; Okamura, M. & Haruta, M. Hydrogen Dissociation by Gold Clusters. *Angew. Chem. Int. Ed.* **48**, 9515-9518 (2009).
3. Nobel prize Sabatier : Paul Sabatier – Nobel Lecture. NobelPrize.org. Nobel Prize Outreach AB 2023. 2023. https://www.nobelprize.org/prizes/chemistry/1912/sabatier/lecture/
4. Hastert, R.C. Hydrogenation of fatty acids. *J Am Oil Chem Soc* 56, 732A–739A (1979).
5. Vogt, C. & Weckhuysen, B.M. The concept of active site in heterogeneous catalysis. *Nat. Rev. Chem.* **6**, 89–111 (2022).
6. Navarro-Jaén, S., Virginie, M., Bonin, J. et al. Highlights and challenges in the selective reduction of carbon dioxide to methanol. *Nat. Rev. Chem.* **5**, 564–579 (2021).
7. Shuo, Ch., Wojcieszak, R., Dumeignil, F., Marceau, E. & Royer, S. How Catalysts and Experimental Conditions Determine the Selective Hydroconversion of Furfural and 5-Hydroxymethylfurfural. *Chem. Rev*. **118**, 11023-11117 (2018).
8. Zugic, B., Wang, L., Heine, C. et al. Dynamic restructuring drives catalytic activity on nanoporous gold–silver alloy catalysts. *Nature Mater.* **16**, 558–564 (2017).
9. Hvolbæk, B. et al. Catalytic activity of Au nanoparticles. *Nano Today* **2**, 14–18 (2007).
10. Fujita, T., Guan, P. & McKenna, K. et al. Atomic origins of the high catalytic activity of nanoporous gold. *Nature Mater.* **11**, 775–780 (2012).
11. Wang, H., Wang, L., Lin, D. et al. Strong metal–support interactions on gold nanoparticle catalysts achieved through Le Chatelier's principle. *Nat. Catal.* **4**, 418–424 (2021).
12. Lopez, N. et al. On the origin of the catalytic activity of gold nanoparticles for low-temperature CO oxidation. *J. Catal.* **223**, 232–235 (2004).
13. Qian, H.; Zhu, M.; Wu, Z.; & Jin, R. Quantum Sized Gold Nanoclusters with Atomic Precision. *Acc. Chem. Res*. **45**, 1470-1479 (2012).
14. Haruta, M. When Gold Is Not Noble: Catalysis by Nanoparticles. *Chem. Rec*. **3**, 75–87 (2003).

15. Corma A. & Garcia, H. Supported gold nanoparticles as catalysts for organic reactions. *Chem. Soc. Rev*. **37**, 2096-2126 (2008).
16. Bond, G.C. Hydrogenation by gold catalysts: an unexpected discovery and a current assessment. *Gold Bull.* **49**, 53–61 (2016).
17. Delgado, J.A. & Godard, C. (2020). Progress in the Selective Semi-hydrogenation of Alkynes by Nanocatalysis. In: van Leeuwen, P., Claver, C. (eds) Recent Advances in Nanoparticle Catalysis. Molecular Catalysis, vol 1. Springer, Cham. https://doi.org/10.1007/978-3-030-45823-2_10
18. Hutchings, G. Heterogeneous Gold Catalysis. *ACS Cent. Sci.* **4**, 1095–1101, (2018).
19. Bus, E., Miller, J.T. & van Bokhoven, J.A. Hydrogen Chemisorption on Al_2O_3-Supported Gold Catalysts. *J. Phys. Chem. B* **109**, 14581–14587 (2005).
20. Green, I.X., Tang, W., Neurock, M.& Yates, J.T. Low-Temperature Catalytic H_2 Oxidation over Au Nanoparticle/TiO_2 Dual Perimeter Sites. *Angew. Chem. Int. Ed.* **50**, 10186–10189 (2011).
21. Manzoli, M., Chiorino, A., Vindigni, F. & Boccuzzi, F. Hydrogen interaction with gold nanoparticles and clusters supported on different oxides: A FTIR study. *Catal. Today* **181**, 62–67 (2012).
22. Boronat, M., Concepcion, P. & Corma, A. Unravelling the Nature of Gold Surface Sites by Combining IR Spectroscopy and DFT Calculations. Implications in Catalysis. *J. Phys. Chem. C* **113**, 16772–16784 (2009).
23. Watkins, W.L. & Borensztein, Y. Mechanism of hydrogen adsorption on gold nanoparticles and charge transfer probed by anisotropic surface plasmon resonance. *Phys. Chem. Chem. Phys*. **19**, 27397-27405 (2017).
24. Hammer, B. & Norskov, J. Why gold is the noblest of all the metals. *Nature* **376**, 238–240 (1995).
25. Sun, X., Dawson, S.R. & Parmentier, T.E. et al. Facile synthesis of precious-metal single-site catalysts using organic solvents. *Nat. Chem.* **12**, 560–567 (2020).
26. Guan, Q., Zhu, C., Lin, Y. et al. Bimetallic monolayer catalyst breaks the activity–selectivity trade-off on metal particle size for efficient chemoselective hydrogenations. *Nat. Catal.* **4**, 840–849 (2021).
27. Chmielewski, A. et al. Reshaping Dynamics of Gold Nanoparticles under H_2 and O_2 at Atmospheric Pressure. *ACS Nano* **13 (2)**, 2024-2033, (2019).
28. Bai, S.T., De Smet, G., Liao, Y. et al. Homogeneous and heterogeneous catalysts for hydrogenation of CO_2 to methanol under mild conditions. *Chemical Society Reviews* **50**, 4259-4298 (2021).
29. Gesesse D., Wang, C., Chang Bor, K., Tai S-H. et al. A soft-chemistry assisted strong metal–support interaction on a designed plasmonic core–shell photocatalyst for enhanced photocatalytic hydrogen production. *Nanoscale* **12**, 7011-7023 (2020).
30. Ferraz P, C., Navarro-Jaén, S., Rossi, L. et al. Enhancing the activity of gold supported catalysts by oxide coating: towards efficient oxidations. *Green Chemistry* **23**, 8453-8457, (2021).
31. Nguyen, K.T., Hiep Vuong, V., Nguyen, T.N. et al. Unusual hydrogen implanted gold with lattice contraction at increased hydrogen content. *Nat. Commun.* **12**, 1560 (2021).

32. Luza, L., Rambor, C., Gual, A., Alves Fernandes, J., Eberhardt, D., Dupont, J., Revealing Hydrogenation Reaction Pathways on Naked Gold Nanoparticles. ACS Catal. **7**, 2791–2799 (2017).
33. Luza, L., Gual, A., Alves Fernandes, J., Eberhardt, D., Dupont, J., Tunneling effects in confined gold nanoparticle hydrogenation catalysts. *Phys. Chem. Chem. Phys*., **21**, 16615-16622 (2019).
34. Martín, A.J., Mitchell, S., Mondelli, C. et al. Unifying views on catalyst deactivation. *Nat. Catal.* **5**, 854–866 (2022).
35. Segura, Y., Lopez, N. & Perez-Ramirez, J. Origin of the superior hydrogenation selectivity of gold nanoparticles in alkyne + alkene mixtures: Triple- versus double-bond activation. *J. Catal.* **247,** 383-386 (2007).
36. van Deelen, T. W., Hernández Mejía, C. & de Jong, K. P. Control of metal-support interactions in heterogeneous catalysts to enhance activity and selectivity. *Nat. Catal.* **2**, 955–970 (2019).
37. Vijay, S., Ju, W., Brückner, S. et al. Unified mechanistic understanding of CO_2 reduction to CO on transition metal and single atom catalysts. *Nat. Catal.* **4**, 1024–1031 (2021).
38. Nørskov, J., Bligaard, T., Rossmeisl, J. et al. Towards the computational design of solid catalysts. *Nature. Chem.* **1**, 37–46 (2009). 39
39. Milone, C., Ingoglia, R., Pistone, A., Neri, G., Frusteri, F. & Galvagno, S. Selective hydrogenation of *α,β*-unsaturated ketones to *α,β*-unsaturated alcohols on gold-supported catalysts. *J. Catal.* **222**, 348-356 (2004).
40. Silva, R., Fiorio, J., Vidinha, P., Rossi, L.M., Gold Catalysis for Selective Hydrogenation of Aldehydes and Valorization of Bio-Based Chemical Building Blocks. *J. Braz. Chem. Soc*., **30**, 2162-2169 (2019).
41. Fiorio, J. & Rossi, L. Clean protocol for deoxygenation of epoxides to alkenes *via* catalytic hydrogenation using Au. *Catal. Sci. Technol.* **11**, 312-318 (2021).
42. Fiorio, J., Lopez, N. & Rossi, L. Au–Ligand-Catalyzed Selective Hydrogenation of Alkynes into *cis*-Alkenes via H_2 Heterolytic Activation by Frustrated Lewis Pairs. *ACS Catal.* **7(4)**, 2973–2980 (2017).
43. Whittaker, T., Kumar, S., Peterson, Ch. et al. H_2 Oxidation over Supported Au Nanoparticle Catalysts: Evidence for Heterolytic H_2 Activation at the Metal–Support Interface. *J. Am. Chem. Soc.* **140(48)**, 16469–16487 (2018).
44. Mukherjee, S., Libisch, F. Large, N., et al. Hot Electrons Do the Impossible: Plasmon-Induced Dissociation of H_2 on Au. *Nano Lett.* **13(1)**, 240–247 (2013).
45. Lin, R., Albani, D., Fako, E., Kaiser, S. et al. Design of Single Au Atoms on Nitrogen-Doped Carbon for Molecular Recognition in Alkyne Semi-Hydrogenation. *Angew. Chim. Int. Ed.* **58**, 504-509 (2019).
46. Stephan, D. The broadening reach of frustrated Lewis pair chemistry. *Science* **354**, aaf7229 (2016).
47. Fiorio, J., Gonçalves, R.V., Teixeira-Neto, E. et al. Accessing Frustrated Lewis Pair Chemistry through Robust Au@N-Doped Carbon for Selective Hydrogenation of Alkynes. *ACS Catal.* **8(4)**, 3516–3524 (2018).

48. Lu, G., Zhang, P., Sun, D. et al. Gold catalyzed hydrogenations of small imines and nitriles: enhanced reactivity of Au surface toward H_2 *via* collaboration with a Lewis base. *Chem. Sci.* **5**, 1082-1090 (2014).
49. Almora-Barrios, N., Cano, I., van Leeuwen, P. & Lopez, N. Concerted Chemoselective Hydrogenation of Acrolein on Secondary Phosphine Oxide Decorated Gold Nanoparticles. *ACS Catal.* **7(6)**, 3949–3954 (2017).
50. Lv, X., Lu, G., Wang, Z.Q. et al. Computational Evidence for Lewis Base-Promoted CO_2 Hydrogenation to Formic Acid on Gold Surfaces. *ACS Catal.* **7(7)**, 4519–4526 (2017).
51. Ren, D., He, L., Yu, L., Ding, R.-S. et al. An Unusual Chemoselective Hydrogenation of Quinoline Compounds Using Supported Au Catalysts. *J. Am. Chem. Soc*. **134**, 17592−17598 (2012).
52. Cano, I., Chapman, A. M., Urakawa, A., & van Leeuwen, P. W. N. M. Air-Stable Au Nanoparticles Ligated by Secondary Phosphine Oxides for the Chemoselective Hydrogenation of Aldehydes: Crucial Role of the Ligand. *J. Am. Chem. Soc*. **136**, 2520−2528 (2014).
53. Cano, I., Huertos, M. A., Chapman, A. M., Buntkowsky, G., Gutmann, T., Groszewicz, P. B., & van Leeuwen, P. W. N. M. Air-Stable Gold Nanoparticles Ligated by Secondary Phosphine Oxides as Catalyst for the Chemoselective Hydrogenation of Substituted Aldehydes: a Remarkable Ligand Effect. *J. Am. Chem. Soc*. **137(5)**, 7718−7727 (2015).
54. Garcia-Melchor, M. & Lopez, N. Homolytic Products from Heterolytic Paths in H_2 Dissociation on Metal Oxides: The Example of CeO_2. *J. Phys. Chem. C* **118(20)**, 10921–10926 (2014).
55. Aireddy, D., and Ding, K. Heterolytic Dissociation of H_2 in Heterogeneous Catalysis. *ACS Catal.* **12**, 4707−4723 (2022).
56Lyalin, A. & Taketsugu, T. A computational investigation of H_2adsorption and dissociation on Au nanoparticles supported on TiO_2 surface. *Faraday Discuss.* **152**, 185-201 (2011).
57. Du, X. Huang, Y. Pan, X. et al. Size-dependent strong metal-support interaction in TiO_2 supported Au nanocatalysts. *Nat. Commun.* **11**, 5811 (2020).
58. Fu, Q., Wagner, T., Olliges, S. & Carstanjen, H.-D. Metal-oxide interfacial reactions: encapsulation of Pd on TiO_2 (110). *J. Phys. Chem. B* **109**, 944–951 (2005).
59. Sun, Y., Cao, Y., Wang, L. et al. Gold catalysts containing interstitial carbon atoms boost hydrogenation activity. *Nat. Commun.* **11**, 4600 (2020).
60. Mukherjee, S., Zhou, L., Goodman, A. et al. Hot-Electron-Induced Dissociation of H_2 on Gold Nanoparticles Supported on SiO_2. *J. Am. Chem. Soc.* **136**, 64−67 (2014).
61. Christopher, P., Xin, H., Marimuthu, A. et al. Singular characteristics and unique chemical bond activation mechanisms of photocatalytic reactions on plasmonic nanostructures. *Nature Mater.* **11**, 1044–1050 (2012).
62. Linic, S., Christopher, P., Xin, H., & Marimuthu, A. Catalytic and Photocatalytic Transformations on Metal Nanoparticles with Targeted Geometric and Plasmonic Properties. *Acc. Chem. Res*. **46**, 1890-1899 (2013).
63. Brus, L. Noble Metal Nanocrystals: Plasmon Electron Transfer Photochemistry and Single-Molecule Raman Spectroscopy. *Acc. Chem. Res*. **41**, 1742-1749 (2008).
64. Quiroz, J., Barbosa, E., Araujo, T., Fiorio, J. et al. Controlling Reaction Selectivity over Hybrid Plasmonic Nanocatalysts. *Nano Lett.* **18**, 7289−7297 (2018).

65. Barbosa, E., Fiorio, J., Mou, T., Wang, B., Rossi, L. & Camargo, P. Reaction Pathway Dependence in Plasmonic Catalysis: Hydrogenation as a Model Molecular Transformation. *Chem. Europ. J.* **24**, 12330-12339 (2018).
66. Pyykkö, P. Theoretical Chemistry of Gold. *Angew. Chem.* **43**, 4412-4456 (2004).
67. Pyykkö, P. Relativity, Gold, Closed-Shell Interactions, and $CsAu{\cdot}NH_3$. *Angew. Chem. Int. Ed.* **41**, 3573-3578 (2002).
68. De Vos, D. & Sels, B. Gold Redox Catalysis for Selective Oxidation of Methane to Methanol. *Angew. Chem. Int. Ed.***117**, 30-32 (2005).
69. Guzman, J. Correttin, S. Fierro-Gonzalez, J. et al. CO Oxidation Catalyzed by Supported Au: Cooperation between Gold and Nanocrystalline Rare-Earth Supports Forms Reactive Surface Superoxide and Peroxide Species. *Angew. Chem. Int. Ed*. **44**, 4778-4781 (2005).
70. Jones, C., Taube, D., Ziatdinov, V., Periana, R., Nielsen, R., Oxgaard, J. & Goddard III, W. Selective Oxidation of Methane to Methanol Catalyzed, with C-H Activation, by Homogeneous, Cationic Gold. *Angew. Chem. Int. Ed.* **116**, 4726-4729 (2004).
71. Corma, A. Gonzalez-Arellano, C. Iglesias, M. & Sanchez, F. Gold Nanoparticles and Gold(III) Complexes as General and Selective Hydrosilylation Catalysts. *Angew. Chem. Int. Ed.* **119**, 7966-7968 (2007).
72. Wang, L., Guan, E., Zhang, J. et al. Single-site catalyst promoters accelerate metal-catalyzed nitroarene hydrogenation. *Nat. Commun.* **9**, 1362 (2018).
73. Zhang, L., Ren, Y. at al. Single-atom catalyst: a rising star for green synthesis of fine chemicals. *Nat. Sci. Rev*. **5**, 653–672 (2018).
74. Hannagan, R.T., Giannakakis, G., Flytzani-Stephanopoulos, M. & Sykes, E.Ch. Single-atom alloy catalysis. *Chem. Rev.* **120**, 12044–12088 (2020).
75. Cui, X., Li, W., Ryabchuk, P. et al. Bridging homogeneous and heterogeneous catalysis by heterogeneous single-metal-site catalysts. *Nat. Catal.* **1**, 385–397 (2018).
76. Cao, S., Yang, M., Elnabawy, A.O. et al. Single-atom gold oxo-clusters prepared in alkaline solutions catalyse the heterogeneous methanol self-coupling reactions. *Nat. Chem.* **11**, 1098–1105 (2019).
77. Corma, A., Salnikov, O.G., Barskiy, D.A., Kovtunov, K.V. &Koptyug, I.V. Single-Atom Au Catalysis in the Context of Developments in Parahydrogen-Induced Polarization. *Chem. Eur. J.* **21**, 7012-7015 (2015).
78. Qiao, B., Liang, JX., Wang, A. et al. Ultrastable single-atom gold catalysts with strong covalent metal-support interaction (CMSI). *Nano Res.* **8**, 2913–2924 (2015).
79. Guzman, J. & Gates, B.C. Structure and Reactivity of a Mononuclear Gold-Complex Catalyst Supported on Magnesium Oxide. *Angew. Chem. Int. Ed.* **115**, 115-714 (2003).
80. Comas-Vives, A.; Gonzalez- Arellano, C., Corma, A., Iglesias, M. et al. Single-Site Homogeneous and Heterogenized Gold(III) Hydrogenation Catalysts: Mechanistic Implications. *J. Am. Chem. Soc*. **128**, 4756-4765 (2006).
81. Sárkány, A., Schay, Z., Frey, K., Széles, É., Sajó I. Some features of acetylene hydrogenation on Au-iron oxide catalyst. *Appl. Catal. A. Gen*. **380**, 133-141 (2010).
82. Zhang, X., Shi, H., & Xu, B. Catalysis by Gold: Isolated Surface Au^{3+} Ions are Active Sites for Selective Hydrogenation of 1,3-Butadiene over Au/ZrO_2 Catalysts. *Angew. Chem. Int. Ed*. **44**, 7132-7135 (2005).

83. He, X., He, Q., Deng, Y. et al. A versatile route to fabricate single atom catalysts with high chemoselectivity and regioselectivity in hydrogenation. *Nat. Commun.* **10**, 3663 (2019).
84. Single atom catalysts push the boundaries of heterogeneous catalysis. *Nat. Commun.* **12**, 5884 (2021).
85. Wang, Z., Gu, L., Song, L., Wang, H. & Yu, R. Facile one-pot synthesis of MOF supported gold pseudo-single-atom catalysts for hydrogenation reactions. *Mater. Chem. Front.* **2**, 1024-1030 (2018).
86. Liu, J., Zou, Y., Cruz, D. et al. Ligand–Metal Charge Transfer Induced *via* Adjustment of Textural Properties Controls the Performance of Single-Atom Catalysts during Photocatalytic Degradation. *ACS Appl. Mater. Interf.* **13(22)**, 25858–25867 (2021).
87. Vilé, G., Di Liberto, G., Tosoni, S. et al. Azide-Alkyne Click Chemistry over a Heterogeneous Copper-Based Single-Atom Catalyst. A*CS Catal.* **12(5)**, 2947–2958 (2022).
88. Gan, T., He, Q., Zhang, H. et al. Unveiling the kilogram-scale gold single-atom catalysts via ball milling for preferential oxidation of CO in excess hydrogen. *Chem. Eng. J.* **389**, 124490, (2020)
89. Greeley, J.& Mavrikakis, M. Alloy catalysts designed from first principles. *Nature Mater.* **3**, 810–815 (2004).
90. Fu, Q. & Luo, Y. Catalytic Activity of Single Transition-Metal Atom Doped in Cu(111) Surface for Heterogeneous Hydrogenation. *J. Phys. Chem. C* **117**, 14618−14624 (2013).
91. Alayoglu, S., Nilekar, A., Mavrikakis, M. et al. Ru–Pt core–shell nanoparticles for preferential oxidation of carbon monoxide in hydrogen. *Nature Mater.* **7**, 333–338 (2008).
92. Eom, N., Messing, M., Johansson, J., Deppert, K., General Trends in Core–Shell Preferences for Bimetallic Nanoparticles. *ACS Nano* **15**, 8883–8895 (2021).
93. Ledendecker, M., Paciok, P., Osowiecki, W.T. et al. Engineering gold-platinum core-shell nanoparticles by self-limitation in solution. *Commun Chem* **5**, 71 (2022).
94. Venkatachalam, S., Jacob, T. Hydrogen Adsorption on Pd- Containing Au(111) Bimetallic Surfaces. *Phys. Chem. Chem. Phys.* **11(17)**, 3263-3270 (2009).
95. van der Hoeven, J.E.S., Tong Ngan, H., Taylor, A., Eagan, N., Aizenberg, J., Sautet, Ph., Madix, R., Friend, C., Entropic Control of H–D Exchange Rates over Dilute Pd-in-Au Alloy Nanoparticle Catalysts. *ACS Catal.* **11**, 12, 6971–6981 (2021).
96. van der Hoeven, J.E.S., Jelic, J., Olthof, L.A. et al. Unlocking synergy in bimetallic catalysts by core–shell design. *Nat. Mater.* **20**, 1216–1220 (2021).
97. Luneau, M., Guan, E., Chen, W. et al. Enhancing catalytic performance of dilute metal alloy nanomaterials. *Commun Chem* **3**, 46 (2020).
98. Bruno, L., Scuderi, M., Priolo, F. et al. Enlightening the bimetallic effect of Au@Pd nanoparticles on Ni oxide nanostructures with enhanced catalytic activity. Sci Rep 13, 3203 (2023).
99. Zhao, J., Ni, J., Xu, J., Cen, J., Li, X. Ir promotion of TiO_2 supported Au catalysts for selective hydrogenation of cinnamaldehyde. *Catal. Comm.* **54**, 72-76 (2014).
100. Li, H., Zheng, J., Zheng, X., Gu, Z., Yuan, Y., Yang, Y. Improved chemoselective hydrogenation of crotonaldehyde over bimetallic AuAg/SBA-15 catalyst. *J. Catal.* **330**, 135-144 (2015).

101. Chen, J., Sun, W., Wang, Y., Fang, W. Performant Au hydrogenation catalyst cooperated with Cu-doped Al2O3 for selective conversion of furfural to furfuryl alcohol at ambient pressure. *Green Energy & Envi.***6**, 546-556 (2021).
102. Zhang, X., Han, S., Zhu, B. et al. Reversible loss of core–shell structure for Ni–Au bimetallic nanoparticles during CO_2 hydrogenation. *Nat. Catal.* **3**, 411–417 (2020).
103. Tkachenko, G., Truong, V.G., Esporlas, C.L. et al. Evanescent field trapping and propulsion of Janus particles along optical nanofibers. *Nat Commun* **14**, 1691 (2023)
104. Kyriakou, G., Boucher, M. B., Jewell, A. D., Lewis, E. et al. Isolated Metal Atom Geometries as a Strategy for Selective Heterogeneous Hydrogenations. *Science* **335**, 1209-1212 (2012).
105. Boucher, M. B., Zugic, B., Cladaras, G. et al. Single Atom Alloy Surface Analogs in $Pd_{0.18}Cu_{15}$ Nanoparticles for Selective Hydrogenation Reactions. *Phys. Chem. Chem. Phys*. **15**, 12187−12196 (2013).
106. Sankar, M., Dimitratos, N., Miedziak, P. et al. Designing bimetallic catalysts for a green and sustainable future. *Chem. Soc. Rev*. **41**, 8099-8139 (2012).
107. Maroun, F., Ozanam, F., Magnussen, O. M. & Behm, R. J. The Role of Atomic Ensembles in the Reactivity of Bimetallic Electrocatalysts. *Science* **293**, 1811−1814 (2001).
108. Buurmans, I. & Weckhuysen, B. Heterogeneities of individual catalyst particles in space and time as monitored by spectroscopy. *Nature Chem.* **4**, 873–886 (2012).
109. Sambur, J., Chen, TY., Choudhary, E. et al. Sub-particle reaction and photocurrent mapping to optimize catalyst-modified photoanodes. *Nature* **530**, 77–80 (2016).
110. Yin, H., Zheng, LQ., Fang, W. et al. Nanometre-scale spectroscopic visualization of catalytic sites during a hydrogenation reaction on a Pd/Au bimetallic catalyst. *Nat. Catal.* **3**, 834–842 (2020).
111. Lucci, F.; Darby, M.; Mattera, M.; Ivimey, Ch. et al. Controlling Hydrogen Activation, Spillover, and Desorption with Pd− Au Single-Atom Alloys, *J. Phys. Chem. Lett*. **7**, 480−485 (2016).
112. Liu, J., Uhlman, M., Montemore, M. et al. Integrated Catalysis-Surface Science-Theory Approach to Understand Selectivity in the Hydrogenation of 1-Hexyne to 1-Hexene on PdAu Single-Atom Alloy Catalysts. *ACS Catal.* ***9(9)***, 8757–8765 (2019).
113. Shi, D., Sadier, A., Girardon, J.S., Mamede, A.S. et al. Probing the core and surface composition of nanoalloy to rationalize its selectivity: Study of Ni-Fe/SiO_2 catalysts for liquid-phase hydrogenation. *Chem. Catal*. **2(7)**, 1686–1708 (2022).
114. Datye A.K., & Guo, H. Single atom catalysis poised to transition from an academic curiosity to an industrially relevant technology. *Nat. Commun*. **12**, 895 (2021).
115. Zhao, X., Fang, R., Wang, F. *et al.* Atomic design of dual-metal hetero-single-atoms for high-efficiency synthesis of natural flavones. *Nat Commun* **13**, 7873 (2022).
116. Tian, S., Wang, B., Gong, W. *et al.* Dual-atom Pt heterogeneous catalyst with excellent catalytic performances for the selective hydrogenation and epoxidation. *Nat Commun* **12**, 3181 (2021).
117. Zhang, T.; Zheng, P.; Gu, F.; Xu, W. et al. The dual-active-site tandem catalyst containing Ru single atoms and Ni nanoparticles boosts CO_2 methanation. *Appl. Catal. B. Env*. **323**, 122190, (2023).

Figure 1. *Types of H_2 activation on heterogeneous Au catalysts and startegies to enhance H_2 disociation on Au.* ***(a)*** *two different types of H_2 activation that may occur on gold* ***(b)*** *Ligands containg N or P adsorbed on Au surface can heterotically dissociate hydrogen due to the interactions between ligand and hydrogen.* ***(c)*** *Strong Support-Metal Interaction (SMSIs) can modify the electronic properties of Au and provide sufficient energy required ofr hydrogen dissociation. On the Figure 1c one of the example of strong SMSI registred in the case of Au supported on TiO_2. The partial encapsulation of Au can be observed.* ***(d)*** *Schematic representation of hydrogen adsorption and charge distribution on Au induced by hot electrons.* ***(e)*** *schematic representation of Au single atom inside of the C_3N_4 structure (blue cirlces represent N atoms, grey circles are carbon atoms).* ***(f)*** *Alloying Au with other metal such as Pt or Pd permits to obtain highly efficient hydrogenation catalysts. H_2 can easily dissociated on Pd or Pt and then can migrate to Au thanks to spillober phenomenon.*

Figure 2. *Selective hydrogenation on Au catalysts in the presence of ligands and in the case of Au-N-doped catalyst (a) Reaction scheme of the catalytic hydrogenation of phenylacetylene (1a) into styrene (2a) and ethylbenzene (3a). (b) Time course of hydrogenation of phenylacetylene (1a) catalysed by Au/SiO_2 in the presence of piperazine. (c) Time course of hydrogenation of phenylacetylene catalysed by Au@N-doped carbon/TiO_2. (d) Experimental reaction rates vs computed activation energies for H_2 dissociation in a heterolytic mode at the N ligand–Au(111) interface. Black squares refer to amines with two N-heteroatoms and red squares refer to amines with one N-heteroatoms in their structures. (e) Computed reaction energy profile for the hydrogenation of an alkyne on phenanthroline-functionalized Au(111) surface. The inset corresponds to Au(111) surface functionalized with phenanthroline in a configuration parallel (flat) to the surface (surface model A). 1a refers to phenylacetylene and 2a to styrene. (Au = yellow, N = blue, C =gray, H = white). Reprinted with permission from*[42,47] . Part B-C adapted with permission from ref 42, ACS. Part D adapted with permission from ref 47, ACS. Part E reprinted with permission from ref 47, ACS.

Figure 3. Hot electron induced *H–D formation at 23 °C on 1% Au/SiO_2 catalyst.* ***(a)*** *The rate of H–D formation was continuously monitored in real-time under two conditions: with laser excitation (2.4 W/cm², active) and without laser excitation (0.0 W/cm², inactive). During the 10-minute period of laser excitation, the sample experienced a reversible temperature increase of 8 °C, as depicted in the figure, transitioning from 22 to 30 °C.* ***(b)*** *H–D formation rate for 1% Au/SiO_2.* ***(c)*** *H–D formation rate for 1% Au/TiO_2 catalyst. In both cases the same reaction condition were applied with laser excitation of 2.4 W/cm²* [60]*. Any activity was observed in the case of SiO_2 (blue curve) and TiO_2 (purple curve). The size of AuNPs were 5−30 nm and the excitation wavelength ranged from 450 to1000 nm.* Part A-C adapted with permission from ref 60, ACS.

Figure 4. *Au single atom catalysts (Au SACs).* ***(a)*** *Schematic representation of the nitrogen-doped carbon (Au(III)/NC) synthesis and impregnation with $HAuCl_4$ used as Au precursor. Impregnation step performed via incipient wetness impregnation of nitrogen doped carbon (NC) with $HAuCl_4$ in aqua regia solution. Two thermal treatment were applied: activation step in static air (at 473 K) and flowing N_2 (>973 K) for 16 h.Color code as follows Au-yellow, C-gray, N-blue, and Cl-green.*[45] ***(b)*** *Aberration corrected HAADF-STEM (High-angle annular dark-field scanning transmission electron microscopy) micrographs of Au/NC1073 catalyst with Au SACs circled (scale bar of 2 nm)*[45]*;* ***(c)*** *TOF (Turnover frequency) in ethene hydrogenation in function of the single Au–Au coordination number on different MgO supported catalysts containing Au^{3+} and Au clusters*[79]. Part A reprinted with permission from ref 45, Wiley. Part B adapted with permission from ref 45, Wiley. Part C reprinted with permission from ref 79, Wiley.

Figure 5. *Spillover region identification.* ***(a)*** *Reaction scheme of the catalytic hydrogenation of chloronitrobenzenethiol to chloroaminobenzenethiol on Au–Pd bimetallic catalysts at 25°C.* ***(b)*** *Illustration of STM-TERS (Sacanning Tunneling Microscopy coupled with Tip-Enhanced Raman Spectroscopy) employing an Ag tip to investigate hydrogenation products on a Pd/Au bimetallic substrate. The black lines culminating in black circles symbolize the electrical connections used to apply a bias voltage between the tip and the sample. The grey hexatomic rings are benzene rings; the small blue balls represent hydrogen.* ***(c)*** *Intensity of the peak at 1,336 cm^{-1} (NO_2 stretching bond in Raman spectra) in TERS line scan spectra on Pd_{LC}/Au (low Pd coverage on Au surface) The size of the active region is represented by the blue regions. Blue arrows indicate the hydrogen spillover direction*[110] ***(d)*** *The topographic height profile for Pd_{LC}/Au (indicated by the red line) of the surface along the dashed line in the inset of the respective STM images is overlaid with a schematic of the surface structure. In this schematic representation, Au is depicted in yellow shading, while Pd is in grey shading. The blue arrows, accompanied by dots, denote the directions of hydrogen spillover.* ***(e)*** *Intensity of the peak at 1,336 cm^{-1} in TERS line scan spectra on Pd_{HC}/Au (high Pd coverage on Au surface).* ***(f)*** *The topographic height profile for Pd_{HC}/Au.* ***(g)*** *and* ***(h)*** *Reaction rate and selectivity profiles for time-resolved hydrogenation of 1-hexyne over $PdAu\text{-}SAA/SiO_2$ catalysts compared to monometallic Pd/SiO_2 catalyst, respectively. B-F r*eprinted from ref.110, Springer Nature Limited. Part G adapted with permission from ref 112, ACS. Part H reprinted with permission from ref 112, ACS.

***Figure 6**. Morphology in the structure of the bimetallic Au@Pt core–shell nanocatalyst. **(a)**, X-ray diffractometry patterns of monometallic Au and bimetallic Au@Pt systems. The structure of Au core is preserved after Pt shell formation as identified using the diffreaction peaks of Au from JCPDS-4-0784 database **(b)**, Recycling tests for Au@ML-Pt catalyst in chemoselective hydrogenation of chloronitrobenzene at 65°C. The activity of the catalyst is stable during 5 cycles. **(c)** HAADF-STEM image of Au@1ML-Pt catalyst accompanied by the corresponding line intensity profiles along the numbered colored rectangles. These profiles serve to reveal both the interplanar distance and the lattice distance. As depicted in the figure, yellow and blue spheres correspond to the Au core and blues ones to the Pt shell. **(d)** Surface atom arrangement in Au–Ni bimetallic nanoparticle at 600 °C (top image) at 400 °C (bottom image). After thermal treatment at 600°C the alloy structure is formed between Ni and Au. After thermperature decrease to 400°C the dealloying occurs and core-structure is formed. The formation of an alloy at 600°C is responsible for the high selectivity of this catalyst in CO_2 hydrogenationas showed in **(e)** Selectivity and conversion temperature resolved profiles for the Ni-Au bimetallic catalyst. The highest conversion is obtained at 600°C when the alloy structure is formed. (scale bars, 2 nm). **(f)** The energy routes for the CO_2 hydrogenation reaction on the (111) surface of the alloyed Ni–Au phase are depicted. The alloying process and reaction pathways are elucidated through DFT (Density functional theory) calculations and FTIR (Fourier Transform Infrared Spectroscopy), shedding light on the mechanism. In this context, TS represents the transition state.* Part A adapted from ref.26, Springer Nature Limited. Part C reprinted from ref.26, Springer Nature Limited. Parts E&F reprinted from ref.102, Springer Nature Limited. Part D adapted from ref.102, Springer Nature Limited.

BOX 1: The importance of the hydrogenation in chemical industry

Hydrogenation reactions are fundamental processes in the chemical industry with widespread applications. Catalytic hydrogenation process was firstly performed in 1897 by Sabatier who described the reduction of ethylene using metals such as Ni, Co and Fe (1912 Nobel Prize in Chemistry)[3]. The first large scale hydrogenation process was the hydrogenation of fatty acids and their glycerides using Ni catalyst in 1909 in Crosfield, USA[4]. The addition of hydrogen gas (H_2) to a compound in the presence of a catalyst can lead to significant change in the molecular structure of the substrate. One of the most prevalent hydrogenation reactions involves reducing unsaturated compounds. When hydrogen gas reacts with a molecule containing double bonds, these bonds become saturated, leading to the formation of single bonds. This procedure is extensively employed in the production of saturated hydrocarbons, including the conversion of unsaturated vegetable oils into solid fats, such as margarine. In addition to reducing double and triple bonds, hydrogenation reactions are employed in a number of other functional group conversions. For instance, the hydrogenation of carbonyl compounds, such as aldehydes and ketones, leads to the formation of alcohols. This transformation is essential in the production of pharmaceuticals, flavorings, and fragrances. Heterogenous catalytic hydrogenation can be performed using metals such as Ni, Ru, Rh and Pd. In addition, numerous catalytic hydrogenation processes can also be performed on Au-based catalysts, some of which are presented below.

BOX 2: The complexity of the H-Me interactions

Different hydrogen activation pathways can occur on clean-surface Au nanoparticles[32-33], as represented on the figure. The homolytic dissociation of H_2 to atoms on low-coordinated Au atoms is well documented from the theoretical point of view (part a). Depending on the electronegativity of metals, these bonds can more or less polarized. More electronegative metals (such as Au) form mostly covalent bonds with hydrogen (M−H). It is worth noting that chemisorption of hydrogen is almost always exothermic (except on Au and silver surfaces).

Heterolytic dissociation of hydrogen is more commonly observed whereby a metal hydride is formed after proton transfer to the support or substrate (part b). Typically, metal hydrogenation catalysts dissociate H_2 with a proton transfer to a strong conjugate base. This involves the formation of proton−hydride pairs.

A third possibility is the activation of hydrogen molecule with a ligand adsorbed on the Au surface (part c) and the subsequent formation of a new active species (H–L where L = ligand)[32].

Unlike the classical mechanisms of hydrogenation that involve the binding of substrates on the metal surface, a final mechanism, hydrogen transfer, enables the hydrogenation of sterically hindered substrates (part d). This "outer sphere" hydrogenation mechanism involves several steps (adsorption of reactant, adsorption of H_2, complex formation, hydrogen transfer, and desorption) with the overall transformation of a proton transfer to an unsaturated substrate. This mechanism can be used to convert complex molecules, which is useful for the generation of pharmaceutically relevant structures. It also does not require gaseous hydrogen but can employ another liquid hydrogen donor such as ethanol, isopropanol or formic acid[32-33].

Part A-D adapted with permission from ref 32, ACS.

BOX 3: Bimetallic synergy

Bimetallic synergy can substantially improve the catalytic properties of a monometallic catalyst and can even promote new catalytic abilities that are not possible in a monometallic catalyst. The addition of a second metal can alter the activity, selectivity and resistance to deactivation inherent to the monometallic particles. The structure of bimetallic particles differs from bulk alloys, and are categorized into core-shell, mixed and Janus structures (examples of different structures are given on figure below), which is mainly determined by the nature of the metal, molar ratio between both metals and the method used for their synthesis[92]. Bimetallic nanoparticles can experience surface segregation phenomena (distribution of the two different metal on the surface of the nanoparticle is not homogeneous and one of the metals tends to concentrate or segregate on the surface), which are crucial in both the synthesis and applications of these nanoparticles. Au based bimetallic catalysts have been studied in hydrogenation reactions, the most common of which are: Au–Pt[26,93], Au–Pd[94-98], Au–Ir[99], Au–Ag[100], Au–Cu[101], Au–Ni[102] and Au–SiO_2[103].

Summary:

Gold catalysts have gained attention for their ability to activate hydrogen towards the hydrogenation of organic molecules. This review explores strategies to enhance hydrogen-gold interactions to help design new efficient hydrogenation catalysts.

Author notes

Please check these figures carefully and return any comments/amendments that you might have to me as soon as possible. In particular, we would like you to check the following:

- Do the figures convey the intended message?
- Are all the labels accurate and in the correct place?
- Are all the arrows in the right place?
- Are any chemical structures correct?
- Have shapes and colours been used consistently and accurately throughout the figures?
- Please note, the Art Editors use colour to show hierarchy within the figure set. Please check and confirm that the most important parts of the figures have been emphasised correctly
- Have any of the figures been previously published, or have they been supplied by a colleague(s) who is not a named author on the article?
- For any maps, some style modifications may have been made, are they still correct?

To mark up any corrections, please use the commenting tools in the PDF, or print and draw by hand, rather than directly editing the PDFs.

Fig 1

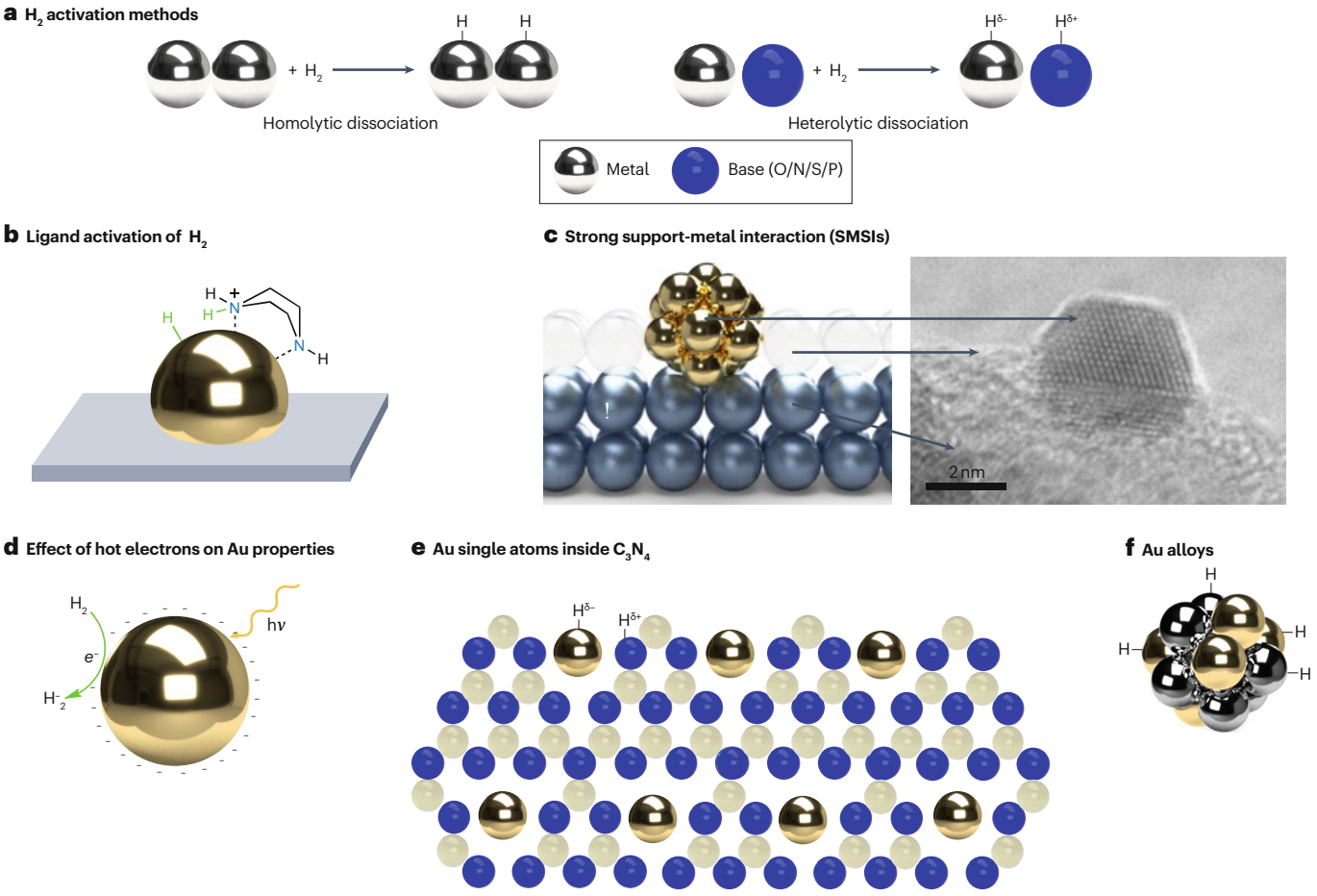
a H2 activation methods
+ H2
H H
Homolytic dissociation
+ H2
Hδ- Hδ+
Heterolytic dissociation
Metal
Base (O/N/S/P)
b Ligand activation of H2
c Strong support-metal interaction (SMSIs)
2 nm
d Effect of hot electrons on Au properties
H2
e-
H-2
hν
e Au single atoms inside C3N4
Hδ-
Hδ+
f Au alloys
H
H
H
H

Fig 2

a Catalytic hydrogenation of phenylacetylene into styrene and ethylbenzene

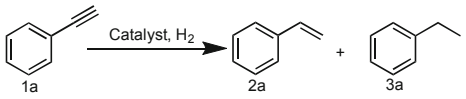

b Reaction course with Au/SiO_2 catalyst and piperazine

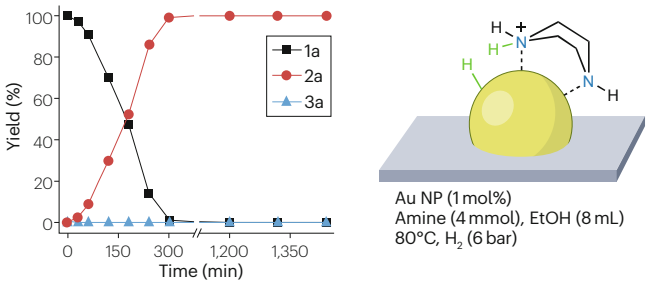

c Experimental reaction rates vs computed activation energies for H_2 dissociation at the N ligand–Au(111) interface

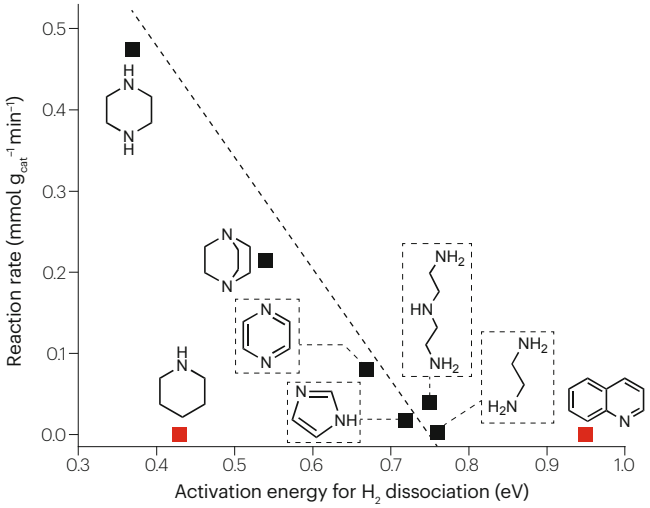

d Reaction course with Au@N-doped carbon/TiO_2 catalyst

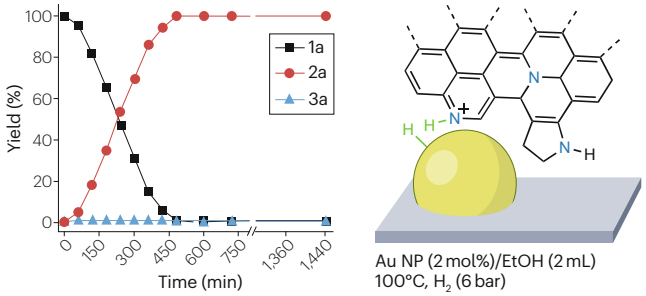

e Computed reaction energy profile for hydrogenation on phenanthroline-functionalized Au(111) surface

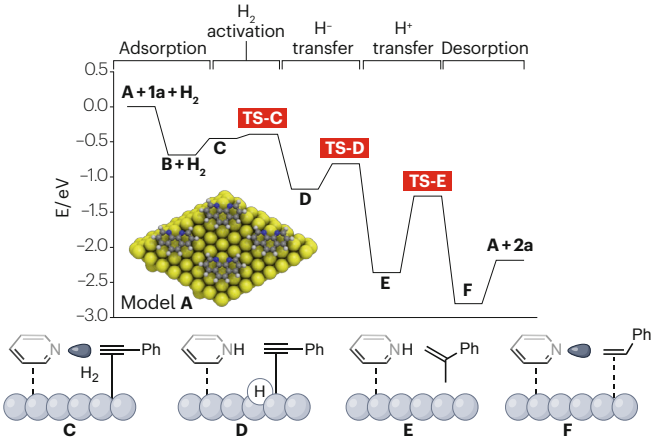

Fig 3

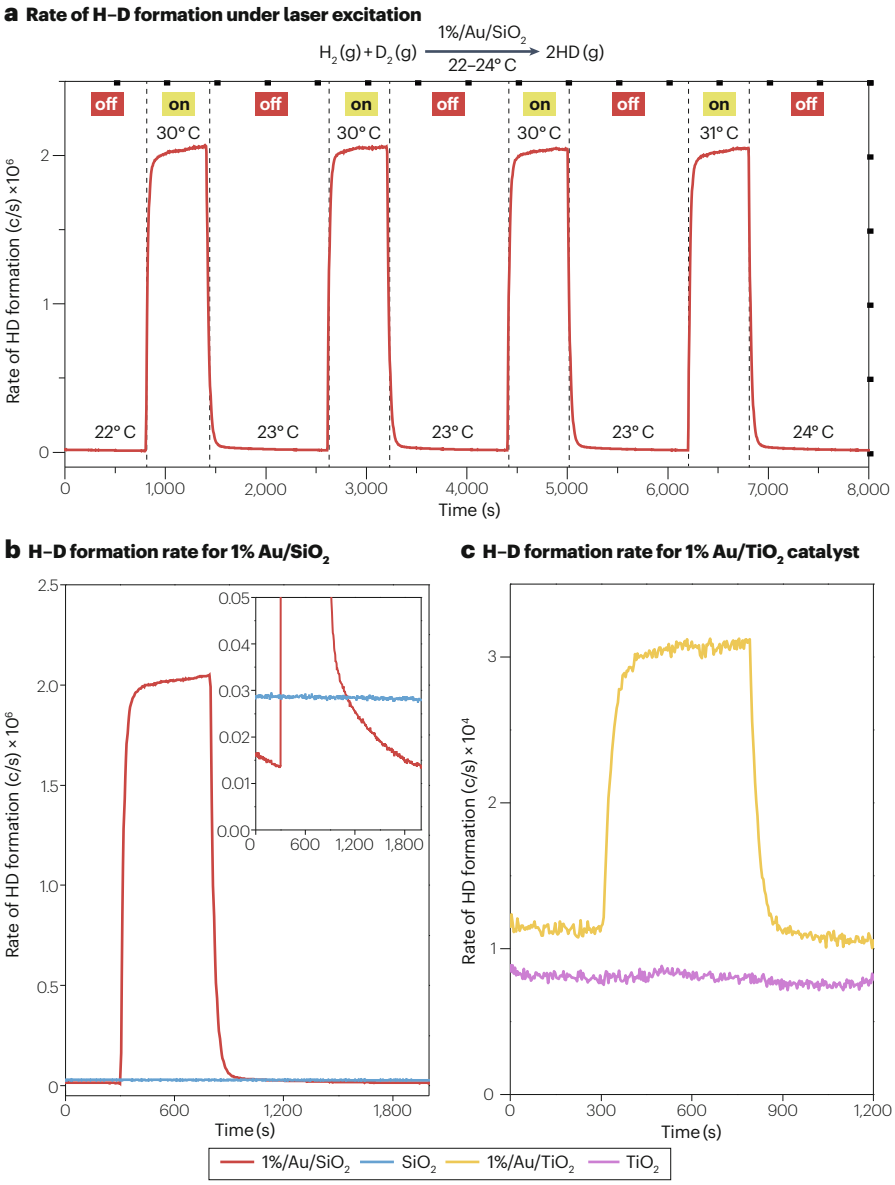
a Rate of H–D formation under laser excitation
H2(g) + D2(g) 1%/Au/SiO2 22–24° C 2HD(g)
off
on
off
on
off
on
off
on
off
30° C
30° C
30° C
31° C
22° C
23° C
23° C
23° C
24° C
Rate of HD formation (c/s) ×10⁶
Time (s)
b H–D formation rate for 1% Au/SiO2
Rate of HD formation (c/s) × 10⁶
Time (s)
c H–D formation rate for 1% Au/TiO2 catalyst
Rate of HD formation (c/s) × 10⁴
Time (s)
1%/Au/SiO2
SiO2
1%/Au/TiO2
TiO2

Fig 4

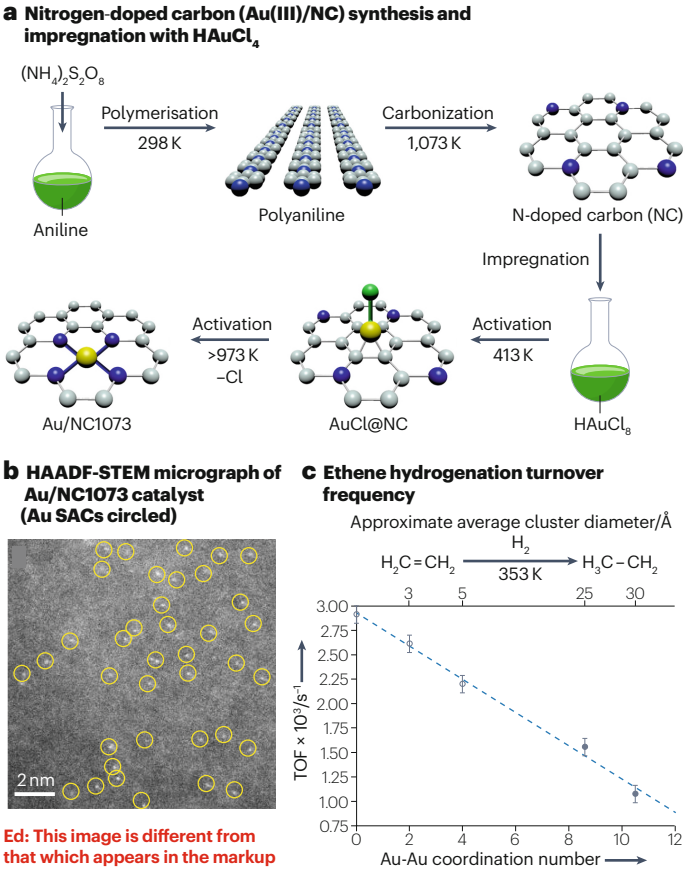

Ed: This image is different from that which appears in the markup

Fig 5

a Catalytic hydrogenation of chloronitrobenzenethiol to chloroaminobenzenethiol

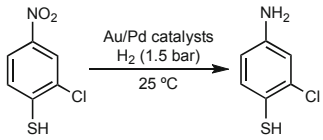

b STM-TERS illustration of an Ag tip investigating hydrogenation on Pd/Au

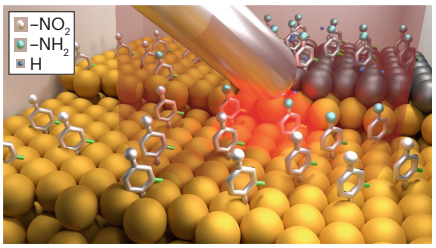

c NO_2 stretching bond (Raman) intensity in TERS line scan spectra on Pd_{LC}/Au

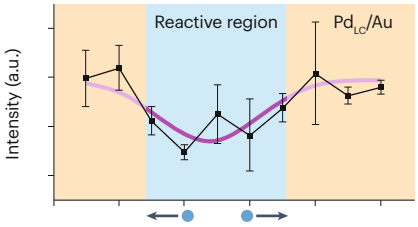

e NO_2 stretching bond (Raman) intensity in TERS line scan spectra on PdHC/Au (high Pd coverage on Au).

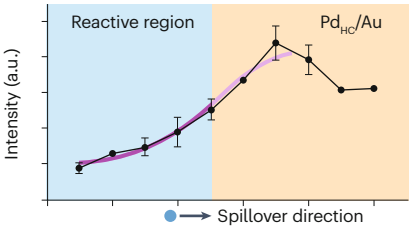

d Topographic height profile for Pd_{LC}/Au

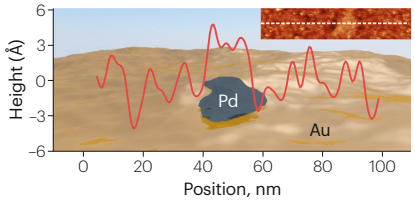

f Topographic height profile for Pd_{HC}/Au

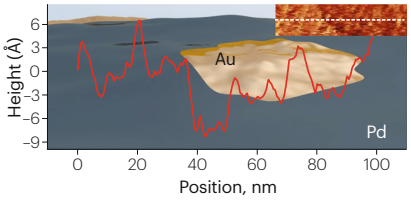

g Reaction rate for time-resolved hydrogenation of 1-hexyne over PdAu-SAA/SiO_2 v. monometallic Pd/SiO_2 catalyst

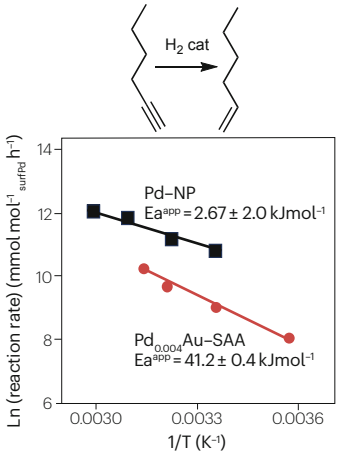

h Selectivity profile

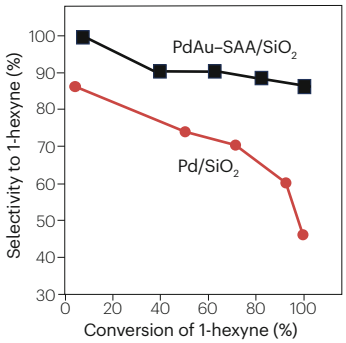

Fig 6

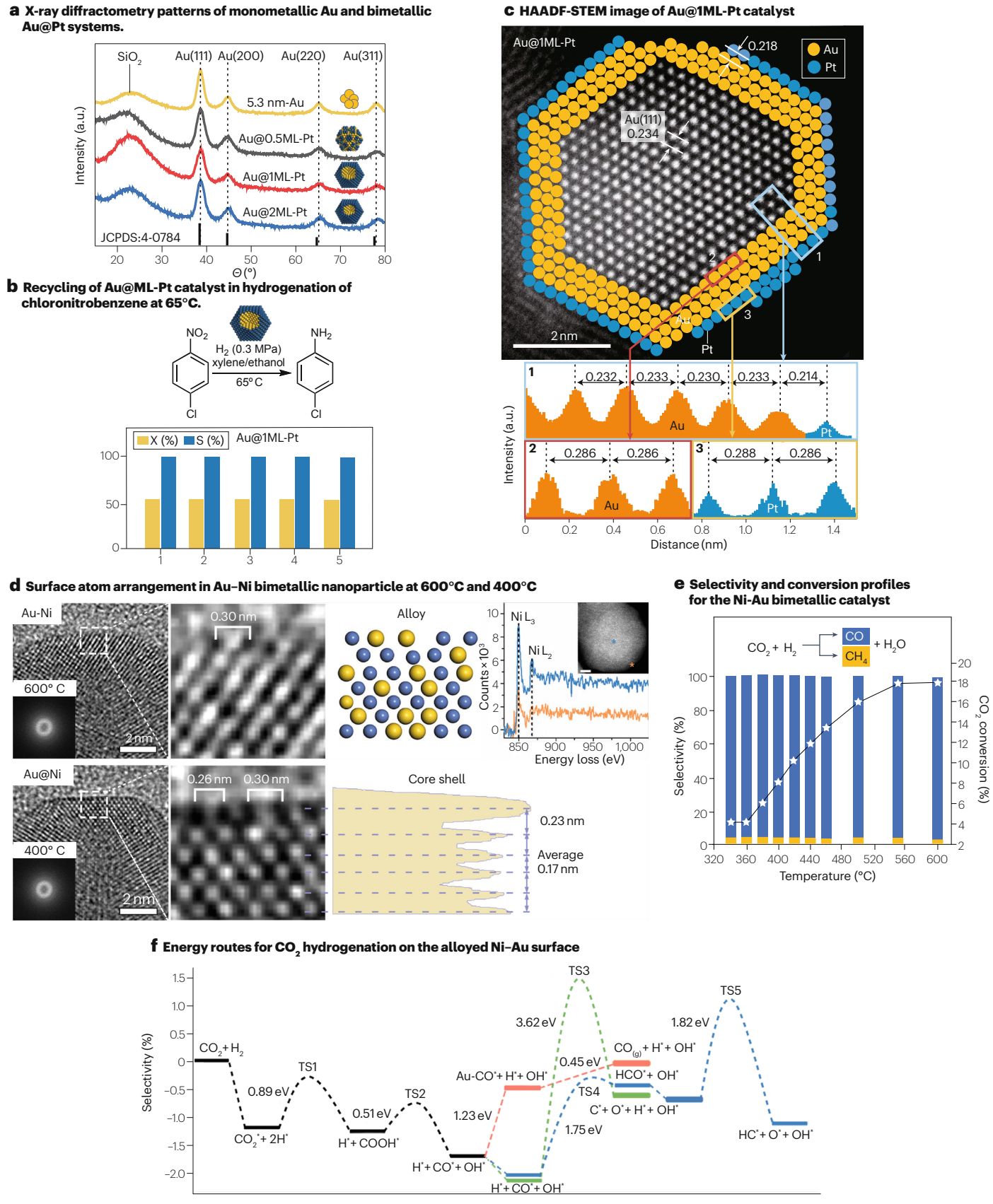
a X-ray diffractometry patterns of monometallic Au and bimetallic Au@Pt systems.
SiO2
Au(111)
Au(200)
Au(220)
Au(311)
5.3 nm-Au
Au@0.5ML-Pt
Au@1ML-Pt
Au@2ML-Pt
JCPDS:4-0784
Intensity (a.u.)
Θ(°)
b Recycling of Au@ML-Pt catalyst in hydrogenation of chloronitrobenzene at 65°C.
NO2
NH2
H2 (0.3 MPa)
xylene/ethanol
65°C
Cl
X (%)
S (%)
Au@1ML-Pt
c HAADF-STEM image of Au@1ML-Pt catalyst
Au@1ML-Pt
0.218
Au
Pt
Au(111)
0.234
2 nm
Intensity (a.u.)
0.232
0.233
0.230
0.233
0.214
0.286
0.286
0.288
0.286
Distance (nm)
d Surface atom arrangement in Au–Ni bimetallic nanoparticle at 600°C and 400°C
Au-Ni
600° C
0.30 nm
2 nm
Alloy
Ni L3
Ni L2
Counts ×10³
Energy loss (eV)
Au@Ni
400° C
0.26 nm
0.30 nm
Core shell
0.23 nm
Average
0.17 nm
e Selectivity and conversion profiles for the Ni-Au bimetallic catalyst
CO2 + H2
CO
CH4
+ H2O
Selectivity (%)
CO2 conversion (%)
Temperature (°C)
f Energy routes for CO2 hydrogenation on the alloyed Ni–Au surface
Selectivity (%)
CO2 + H2
0.89 eV
CO2* + 2H*
TS1
0.51 eV
H* + COOH*
TS2
1.23 eV
H* + CO* + OH*
Au-CO* + H* + OH*
3.62 eV
TS3
H* + CO* + OH*
0.45 eV
TS4
1.75 eV
CO(g) + H* + OH*
HCO* + OH*
C* + O* + H* + OH*
1.82 eV
TS5
HC* + O* + OH*

Box 1

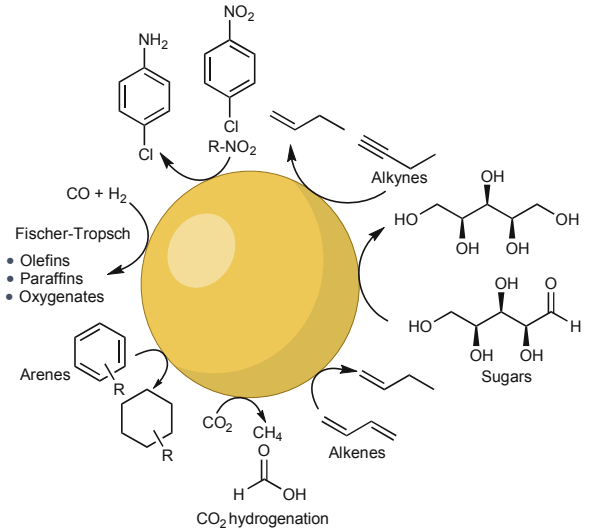

Box 2

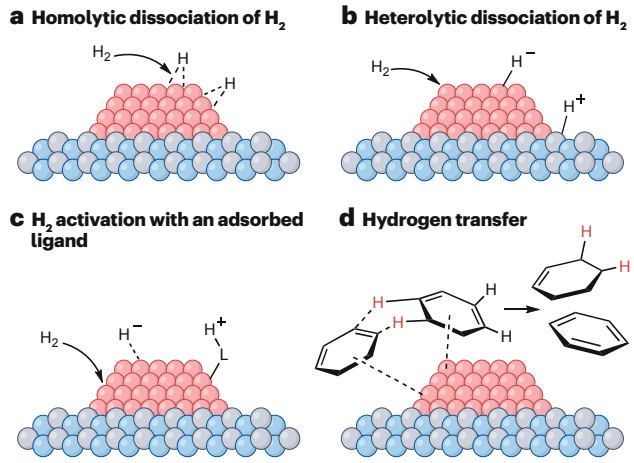

Box 3

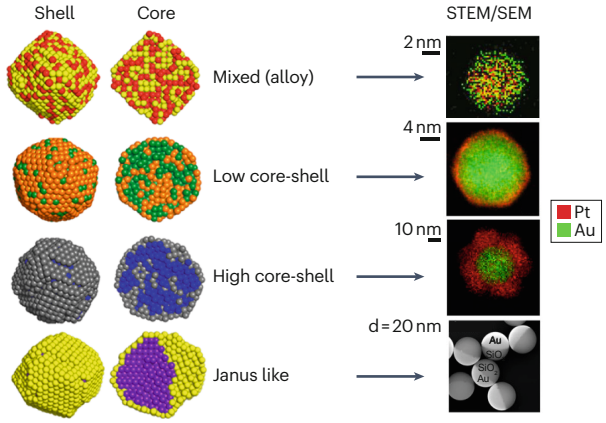

GA